

Search for rare processes in underground laboratories

F. Cappella

Sezione INFN - Roma

Experimental Elementary Particles Physics course

A.A. 2017/18 - Prof. C. Bini

Rare processes

In the search for rare processes, the rate of the searched events that can be measured with the detectors is very low:

from few events per day to few events per year

These events would be completely hidden by the background events if the experiments were not carried out under defined conditions

In particular:

- in underground laboratory to reduce the flux of cosmic rays
- with heavy shields to reduce the contribute of environmental radiation
- with insulating system to eliminate the radon gas contamination
- using selected and purified materials with high radio-purity levels
- with an experimental approach that optimizes the signal/background ratio

Examples of rare processes

□ Very low cross section or flux:

- ✓ **Neutrino** (solar, atmospheric, supernovae, accelerator, reactor, ...)
- ✓ **Dark Matter**
- ✓ Exotic particles in cosmic rays

□ Very long lifetime:

- ✓ **Double beta decays**
- ✓ Rare α and β decays
- ✓ Cluster decays
- ✓ Spontaneous transition of nuclei to a superdense state;
- ✓ Stability of matter (electron or nucleon decay)
- ✓ Processes violating the Pauli exclusion principle
- ✓ Charge non-conserving (CNC) processes
- ✓ Long-lived superheavy elements
- ✓ Many other rare processes of and beyond the Standard Model

Neutrino physics

What we know (from ν oscillations):

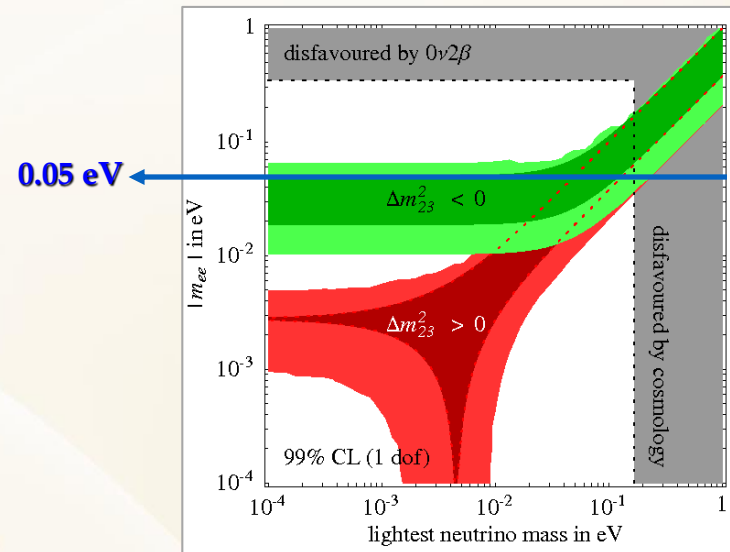
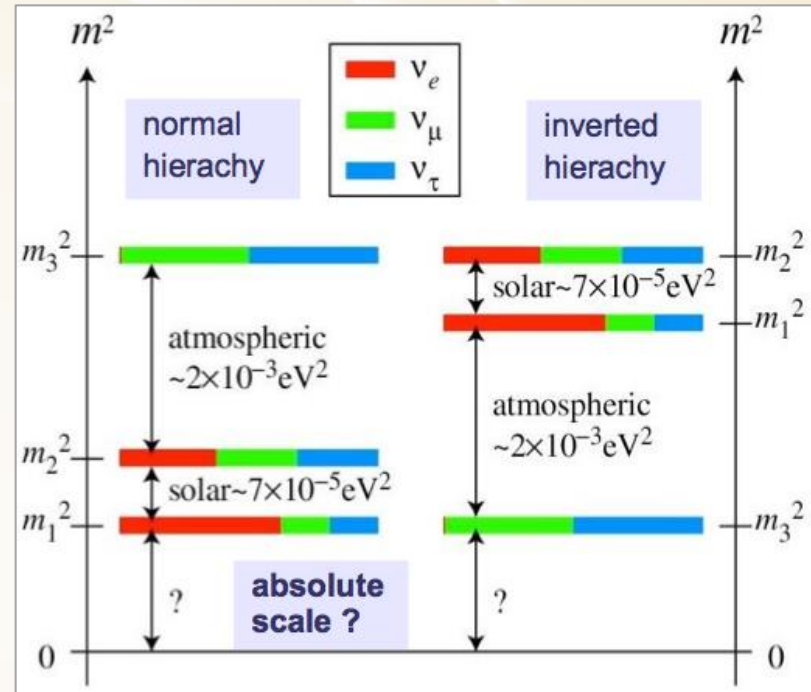
- Neutrino flavour eigenstates differ from their mass eigenstates
- Neutrino oscillate, hence they must have mass
- Mixing angles and Δm^2 values known (with varying accuracies)

What we don't know

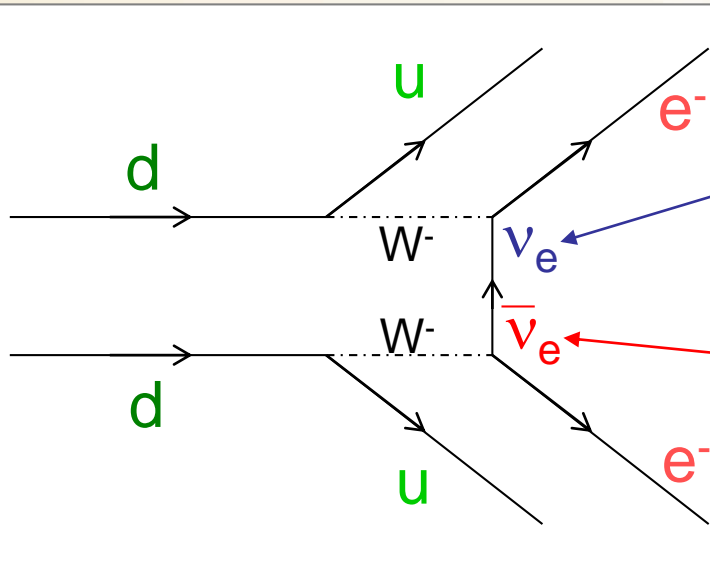
- Normal or inverted hierarchy
- Dirac or Majorana particle?
- CP violating phases in mixing matrix?
- No information about absolute mass scale! (only upper limits)
- Evidence of sterile neutrinos?

How to know

- Neutrino Oscillations
- Double Beta Decay
- Cosmology
- Direct Beta Decay Endpoint



Neutrino properties and 0ν -DBD



a LH neutrino ($L=-1$)
is absorbed at this vertex

a RH antineutrino ($L=1$)
is emitted at this vertex

in pre-oscillations
standard particle physics
(massless neutrinos),
the process is forbidden because
neutrino has not the correct
helicity / lepton number
to be absorbed
at the second vertex

- IF neutrinos are massive **DIRAC** particles:

Helicities can be accommodated thanks to the **finite mass**,
BUT Lepton number is rigorously conserved



**0ν -DBD
is forbidden**

- IF neutrinos are massive **MAJORANA** particles:

Helicities can be accommodated thanks to the **finite mass**,
AND Lepton number is not relevant



**0ν -DBD
is allowed**

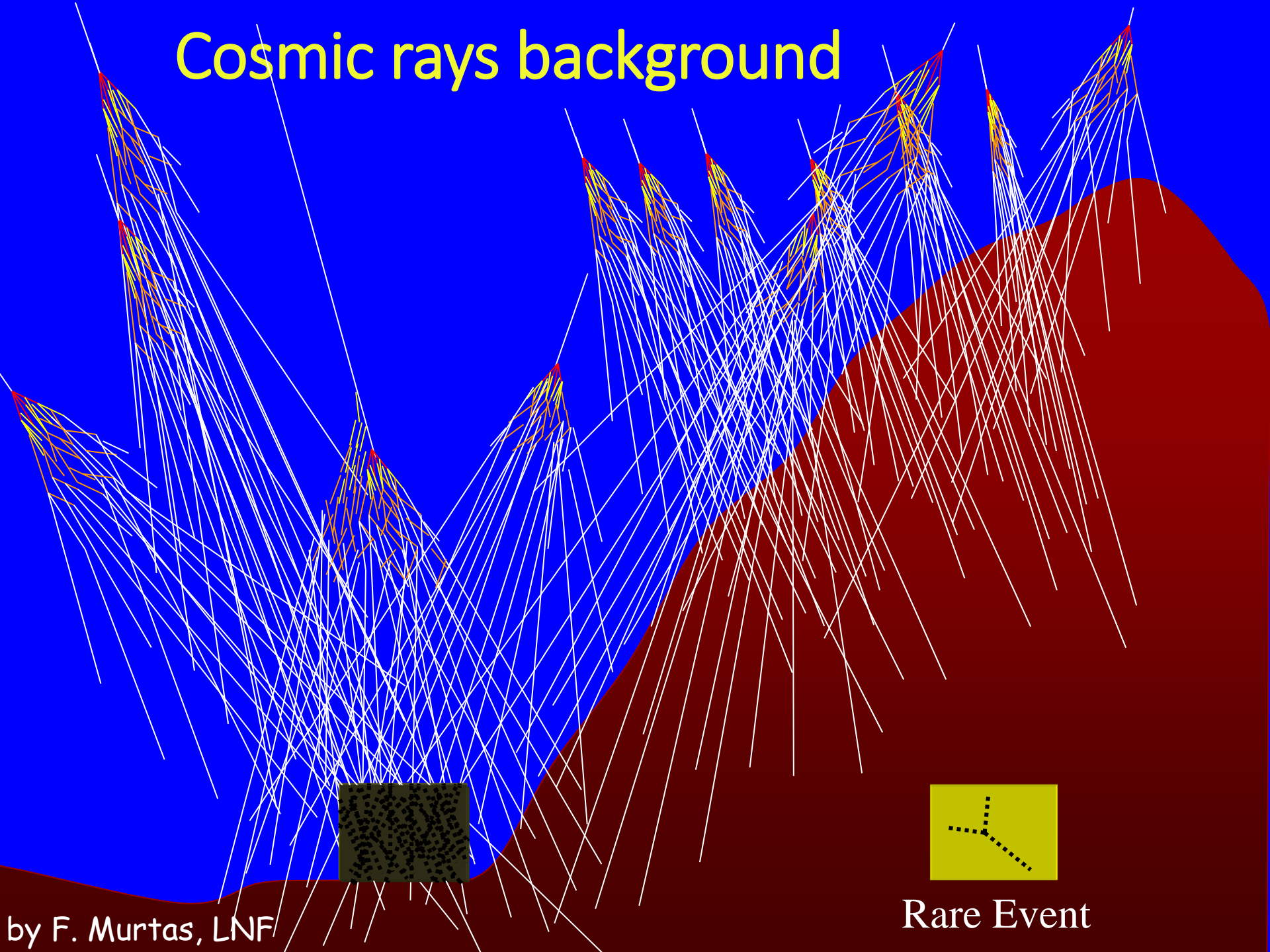
Observation of **0ν -DBD**



$$m_\nu \neq 0$$

$$\bar{\nu} \equiv \nu$$

Cosmic rays background



by F. Murtas, LNF

Rare Event

Primary cosmic rays

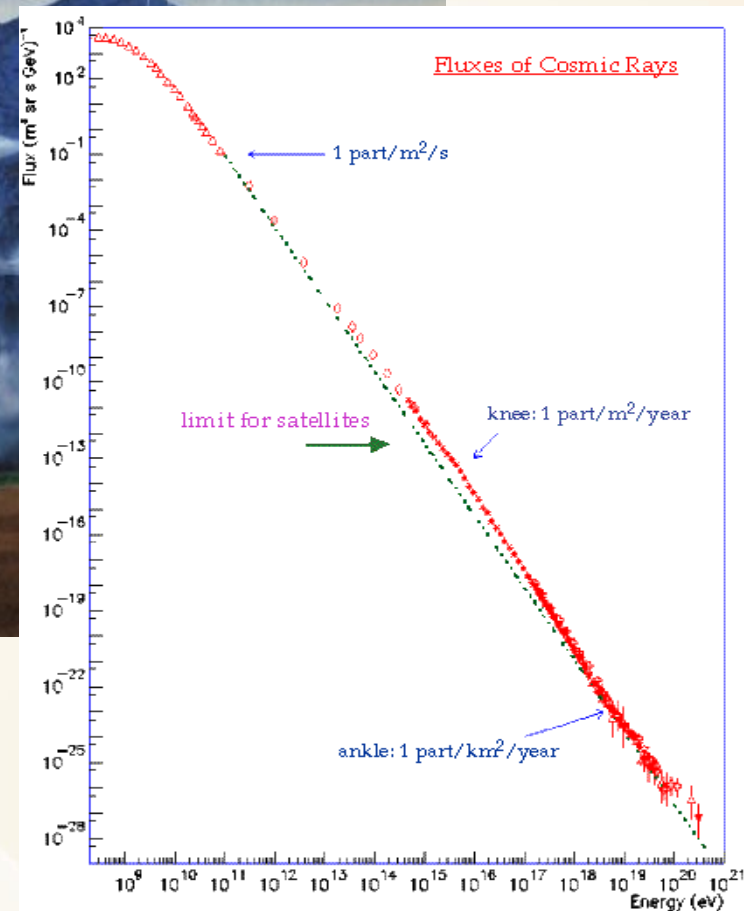
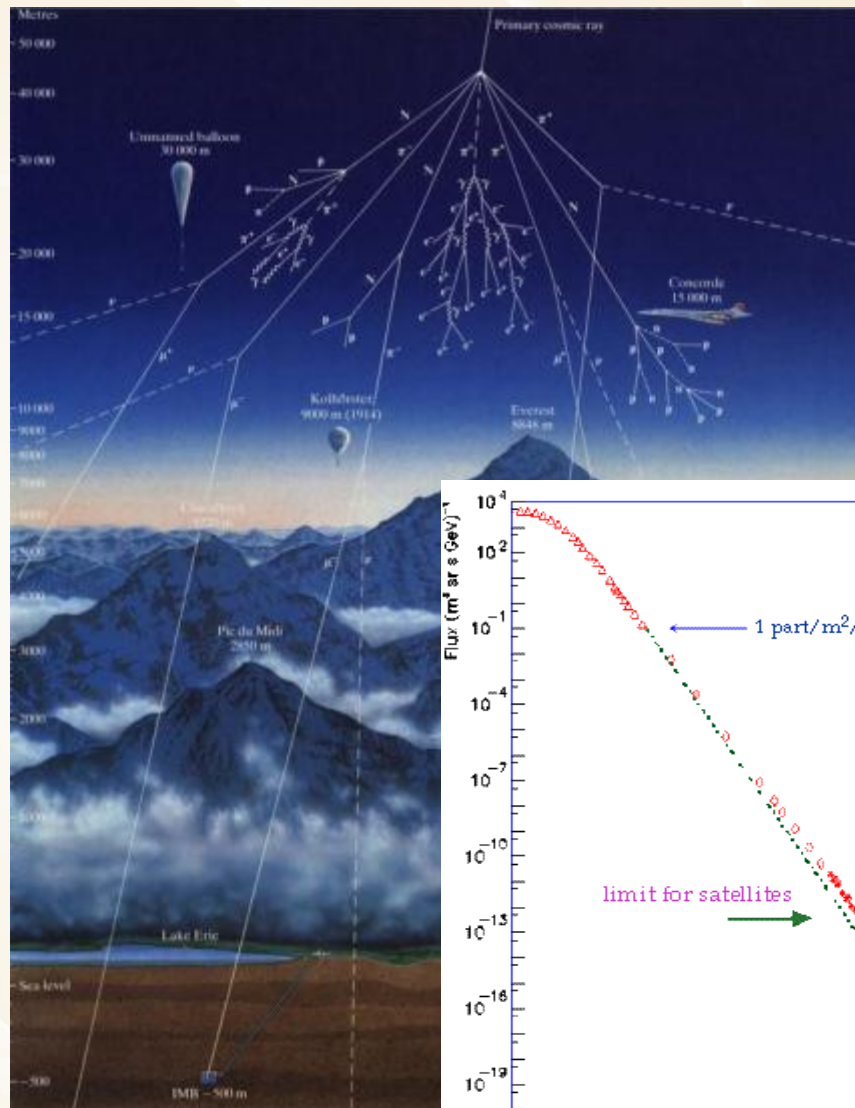
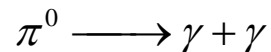
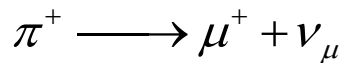
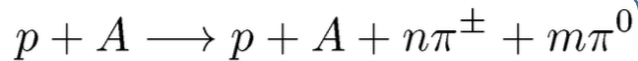
~90% protons, 9% ^4He nuclei, and ~1% heavier particles, hit the earth atmosphere at a rate of about $1000 \text{ m}^{-2} \text{ s}^{-1}$

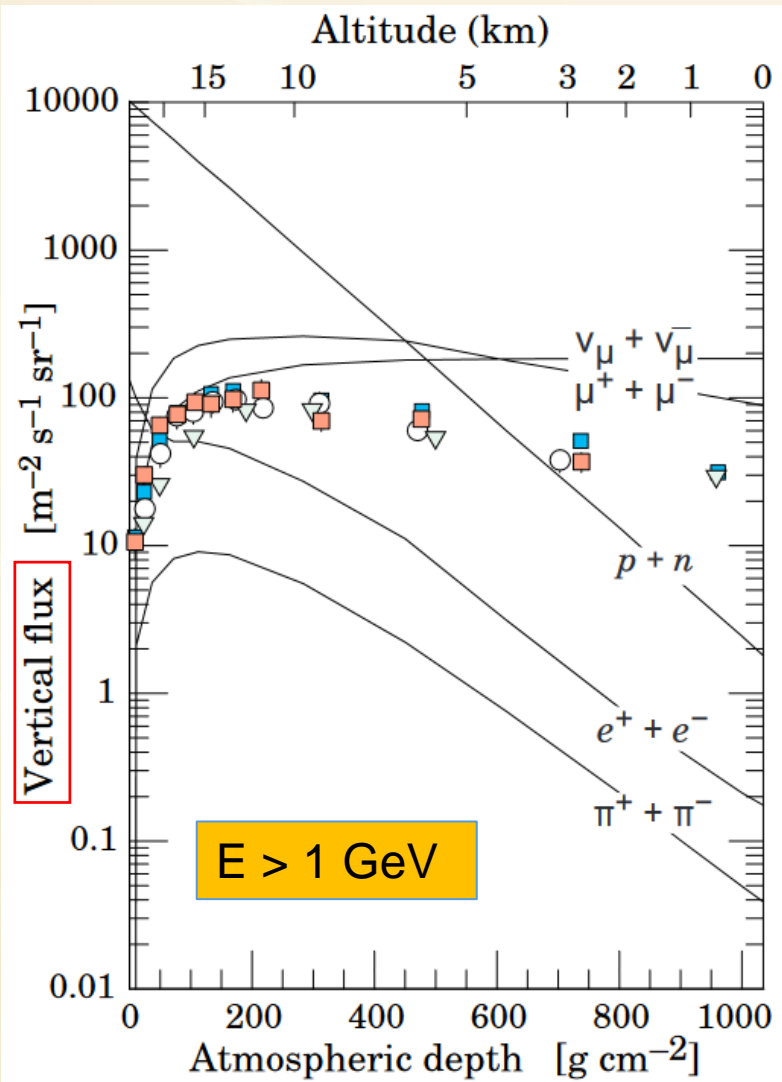
(+ relativistic electrons, X-rays and γ rays and solar and SN neutrinos)

Secondary cosmic rays

The interaction of primary cosmic rays with atmospheric nuclei generates:

- π and k mesons
- muons
- electrons and positrons
- neutrons and secondary protons
- e.m. radiation
- atmospheric neutrinos





Most cosmic radiation that reaches the Earth's surface consists of **muons and neutrinos**

Beyond solar and atmospheric neutrinos, **at sea level**, the secondary radiation is made of **two components**: the soft one and the hard one, that behave differently when passing through dense materials

Hard component (about 70% of the secondary radiation)

- ⇒ Muons, the most numerous charged particles;
 - Their mean energy is ≈ 4 GeV;
 - Their flux is $\approx 1 \text{ cm}^{-2}\text{min}^{-1}$ for horizontal detectors
- ⇒ Depending on their energy muons can penetrate thicknesses of materials from few m to several km (for very high energy muons).

Soft component (about 30% of the secondary radiation)

- ⇒ electrons, positrons, and photons primarily from cascades initiated by decay of neutral and charged mesons. Muon decay is the dominant source of low-energy electrons at sea level
- ⇒ it is able to pass through only a few millimetres of dense material.

Example of cosmic rays reduction in a underground lab

- Muoni
 - 10^6
- Neutroni
 - 10^3
- Fotoni (gamma)
 - 10



LNGS

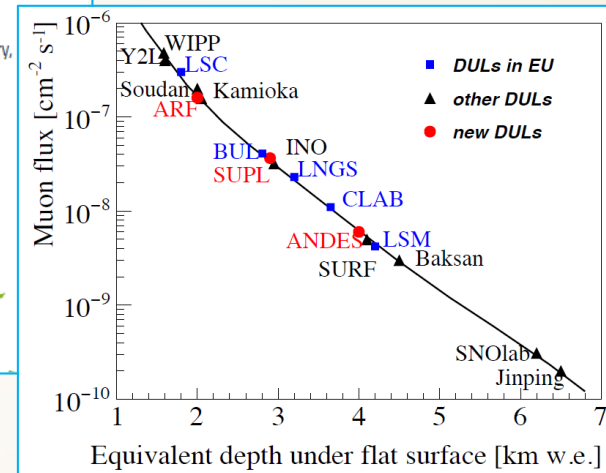
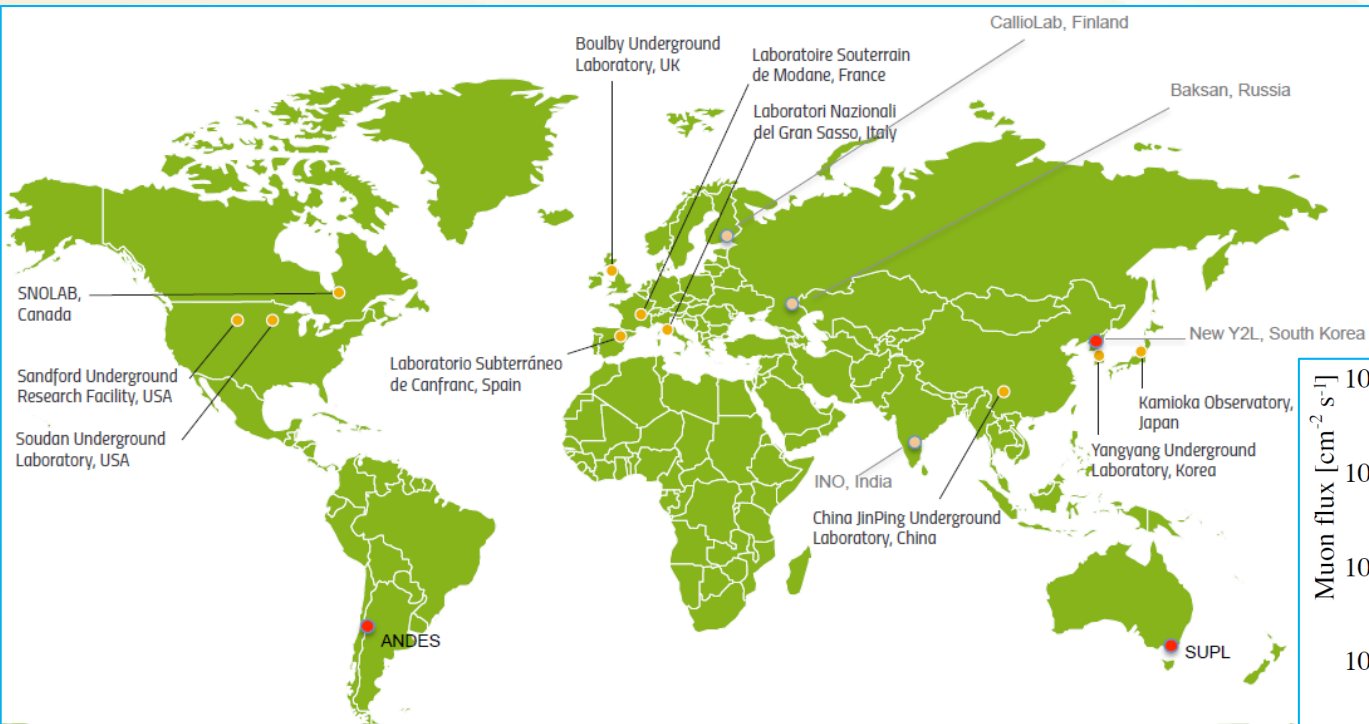
Depth: 1400 m
(**3800 m w.e.**)

Muon Flux

$1.1 \mu \text{ m}^{-2} \text{ h}^{-1}$

Thanks to this cosmic silence, underground laboratories provide the low radioactive background environment necessary to host key experiments to search for extremely rare phenomena in the field of particle and astroparticle physics, nuclear astrophysics and other disciplines

Deep Underground Laboratories (>1000 mwe) in the world



	SNOLab Canada	LNGS Italy	LSC Spain	BUL UK	LSM France	CallioLab Finland	Baksan Russia	SURF USA	CJPL China	Kamioka Japan	Y2L South Korea
since	2003	1987	2010	1989	1982	1995	1967	2007	2009	1983	2003
Volume (m ³)	30000	180000	10000	7200	3500	1000	23000	7160	300000 <i>nearly completed</i>	150000	5000
depth (m)	2070	1400	850	1100	1700	1440	1700	1500	2400	1000	700
access	V	H	H	V	H	V+drive in	H	V	H	H	drive in
Average Rn (Bq/m ³)	130	80	100	<3	15	70	40	300	40	80	40

Underground Laboratories in the world

Europe

- Boulby**: Boulby Palmer Laboratory (UK)
- LNGS**: Laboratorio Nazionale del Gran Sasso (Italy)
- LSC**: Laboratorio Subterráneo de Canfranc (Spain)
- LSM**: Laboratoire Subterrain de Modane (France)
- CallioLab**: Centre for Underground Physics in Pyhäsalmi (Finland)
- Solotvina Underground Laboratory (Ukraine)
- Baksan**: Baksan Neutrino Observatory (Russia)

Asia

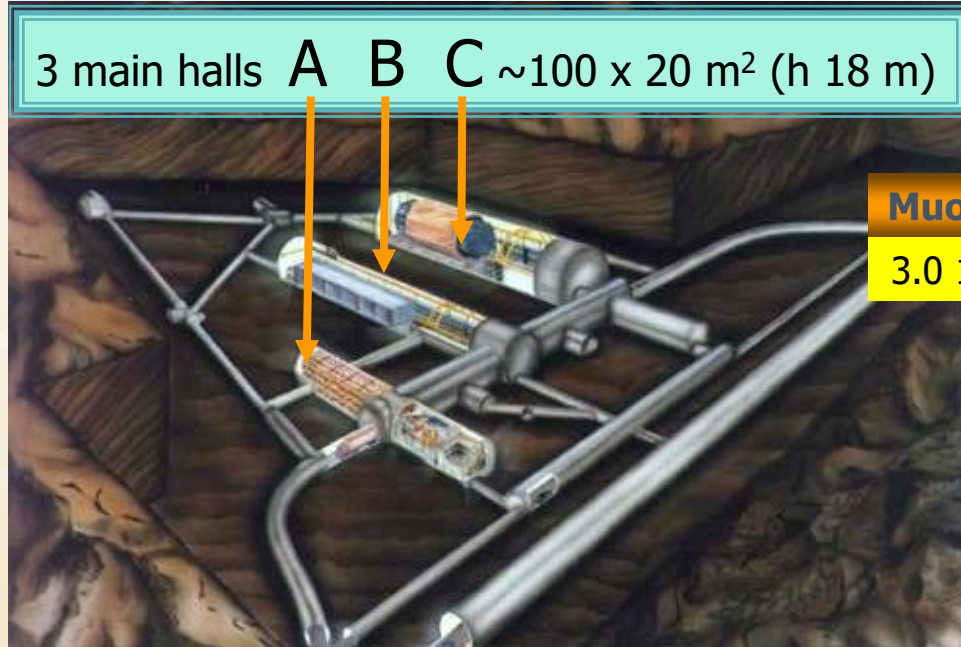
- Y2L**: YangYang Laboratory (Korea)
- Oto Cosmo Observatory (Japan)
- Kamioka**: Kamioka Observatory (Japan)
- INO**: India based Neutrino Observatory (India)
- CJPL**: China Jinping Underground Laboratory (China)

North America

- SNOLab**: Sudbury Neutrino Observatory (Canada)
- SUL**: Soudan Underground Laboratory (USA)
- SURF**: Sanford Underground Research Facility (USA)

Gran Sasso Laboratory

The largest underground laboratory in the world



Currently 1100 scientists from 29 countries are taking part in the experimental activities

Muon Flux

$3.0 \cdot 10^{-4} \mu \text{ m}^{-2} \text{ s}^{-1}$

Neutron Flux

$2.92 \cdot 10^{-6} \text{ n cm}^{-2} \text{ s}^{-1}$ (0-1 keV)

$0.86 \cdot 10^{-6} \text{ n cm}^{-2} \text{ s}^{-1}$ (> 1 keV)

Depth: 1400 m (**3800 m w.e.**)

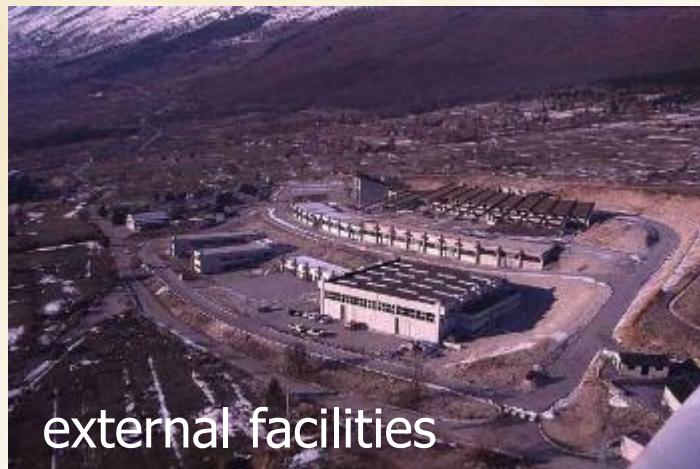
3 halls surface $\sim 6000 \text{ m}^2$

Total surface: 17300 m^2

Volume: **180000 m³**

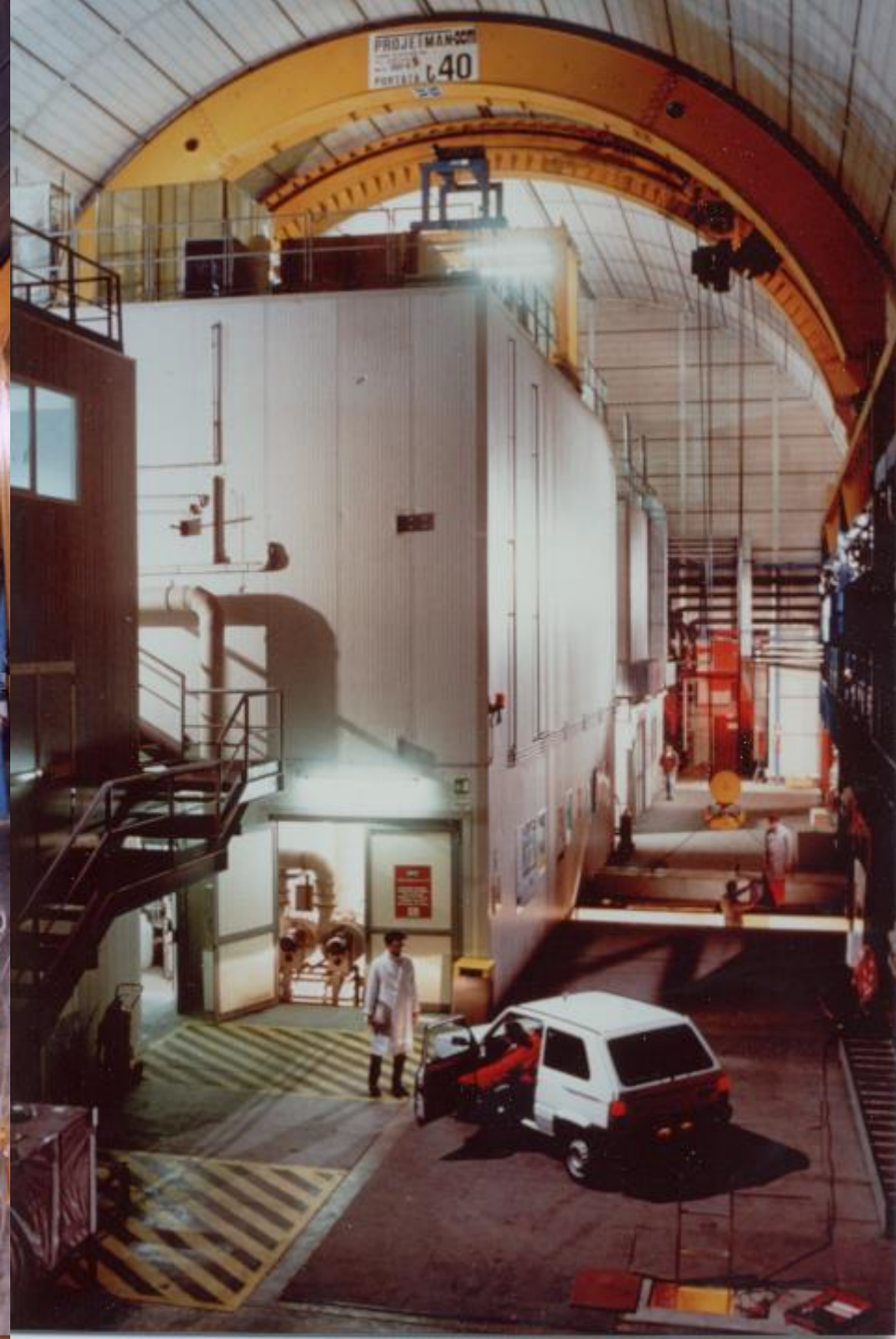
Rn in air: 50-100 Bq/m³

Air-ventilation: 1lab volume/3.5 h



Primordial Radionuclides

^{238}U	0.42 ppm	Rock	(Hall B)
	1.05 ppm	Concrete	All Halls
^{232}Th	0.062 ppm	Rock	(Hall B)
	0.656 ppm	Concrete	All Halls
K	160 ppm	Rock	



Suppression of background

- 1) Underground laboratories
- 2) Shielding against Radon, its progenies and other airborne nuclides
- 3) External shielding
- 4) Material selection for detector construction
- 5) Limitation to the cosmic rays exposure
- 6) Active determination of background (PSD, other bckg identification techniques, id. of a Fiducial Volume ...)
- 7) Coincidence techniques
- 8) Montecarlo simulations

Sources of background

Muon-related background

direct or indirect (via activation of radioactive nuclides and via neutron production)

Neutrons:

- At deep locations the neutron flux is dominated by fission and (α, n) reaction
- The flux of μ -produced neutrons is ~ 3 orders of magnitude lower than that from natural activity, but at higher energy
- Inelastic scattering and radiative capture (n, γ) are the main channels for direct neutron induced background

Radon

The environmental air contains traces of radioactive radon gas, which belong to the U and Th chains. Its daughters attach themselves to surfaces by various processes.

- ^{238}U : ^{222}Rn ($T_{1/2}=3.82$ g)
- ^{232}Th : ^{220}Rn ($T_{1/2}=55.6$ s)
- ^{235}U : ^{219}Rn ($T_{1/2}=3.96$ s)

Environmental radioactivity

External active or passive shielding of the detectors

Radioactive contaminations in detector and shield material

Material screening

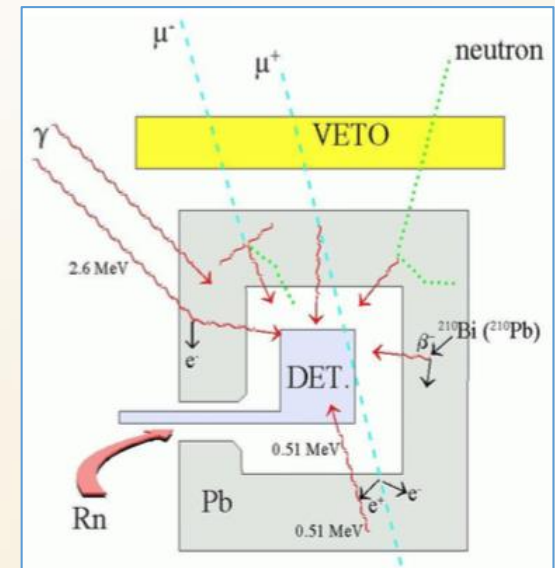
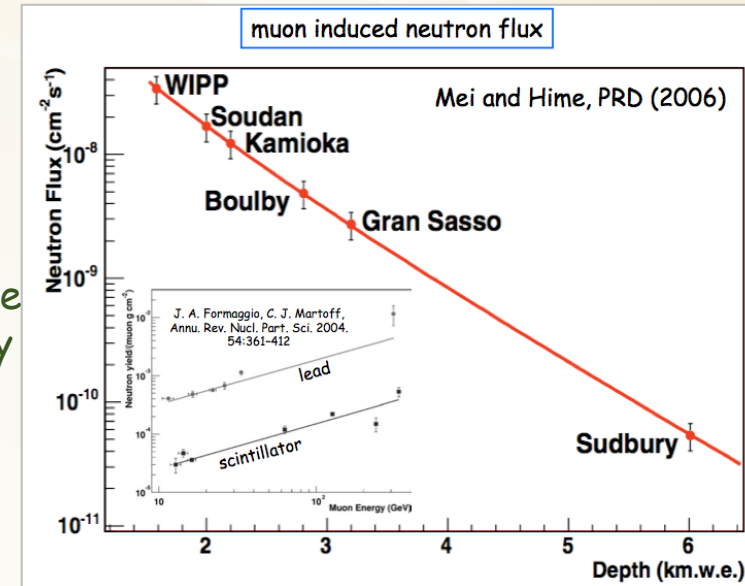
Neutron flux @ LNGS:

thermal $\approx 1.08 \times 10^{-6}$ n cm^{-2} s^{-1}

epithermal $\approx 2 \times 10^{-6}$ n cm^{-2} s^{-1}

fast $\approx 0.9 \times 10^{-7}$ n cm^{-2} s^{-1}

$E_n > 10$ MeV (mostly μ -induced) $\approx 0.5 \times 10^{-9}$ n cm^{-2} s^{-1}



Origin of radioactive contaminations

Fossil radioactivity (present since the formation on the Earth)

- Most elements present on Earth condensed from a interstellar cloud about 4.5×10^9 yr ago.
- This cloud consisted (mostly) of “primordial” ^1H and ^4He produced in the first minutes after the “Big Bang” and heavier elements produced in earlier generations of stars
- At the present epoch, only nuclei with mean lives greater than 10^8 yr are still present in significant numbers

Cosmogenic radioactivity (elements continuously produced by cosmic rays)

Cosmic-rays produce radioactive nuclei via their interactions with nuclei in the atmosphere and in the Earth's crust. \Rightarrow e.g.: the (n,p) reaction on abundant atmospheric nitrogen: $n + ^{14}\text{N} \rightarrow p + ^{14}\text{C}$ $T_{1/2}(^{14}\text{C}) = 5730\text{yr}$

or the “spallation” reactions in a Ge crystal: $n + ^{70}\text{Ge} \rightarrow 3n + ^{68}\text{Ge}$ $T_{1/2}(^{68}\text{Ge}) = 270.7\text{day}$

or for tritium formation in atmosphere: $n + ^{16}\text{O} \rightarrow ^3\text{H} + ^{14}\text{N}$ $T_{1/2}(^3\text{H}) = 12.35\text{yr}$

Artificial radioactivity (due to the development of nuclear technologies)

Fossil radioactivity

These long-lived nuclei involve either highly forbidden β decays (large spin changes) or are α -decays that happen to have Q-values that place the half-lives in this range.

Nuclei with $10^8 \text{ yr} < T_{1/2} < 10^{12} \text{ yr}$

- For the activity in the Earth's crust, the uranium and thorium activities include the activities of the daughters
- Note that three nuclides, ^{40}K , ^{147}Sm and ^{235}U have lifetimes much less than the age of the Earth ($\sim 4.5 \times 10^9 \text{ yr}$) and therefore have very small isotopic abundances

decay	half-life (years)	isotopic abundance (percent)	activity (Bq kg^{-1}) (element)	activity (Bq kg^{-1}) (crust)
$^{40}\text{K} \rightarrow ^{40}\text{Ca} e^- \bar{\nu}_e$ 89% $\rightarrow ^{40}\text{Ar} \nu_e$ 11%	1.28×10^9	0.0117	3.0×10^4	6.3×10^2
$^{87}\text{Rb} \rightarrow ^{87}\text{Sr} e^- \bar{\nu}_e$	4.75×10^{10}	27.83	8.8×10^5	8.0×10^1
$^{146}\text{Sm} \rightarrow ^{142}\text{Nd} \alpha$	1.03×10^8	$< 10^{-7}$	< 1	$< 10^{-4}$
$^{147}\text{Sm} \rightarrow ^{143}\text{Nd} \alpha$	1.06×10^{11}	15.1	1.3×10^5	9×10^{-1}
$^{176}\text{Lu} \rightarrow ^{176}\text{Hf} e^-$	3.78×10^{10}	2.61	5.5×10^4	4×10^{-2}
$^{187}\text{Re} \rightarrow ^{187}\text{Os} e^- \bar{\nu}_e$	4.15×10^{10}	62.6	1.1×10^6	8×10^{-4}
$^{232}\text{Th} \rightarrow ^{228}\text{Ra} \alpha$	1.405×10^{10}	100	4.05×10^6	3.5×10^2
$^{235}\text{U} \rightarrow ^{231}\text{Th} \alpha$	7.038×10^8	0.72	5.7×10^5	1.7×10^1
$^{238}\text{U} \rightarrow ^{234}\text{Th} \alpha$	4.468×10^9	99.275	1.2×10^7	4.7×10^2

The three natural radioactivity chains

uranium series

$^{238}\text{U}_{92}$	4.468 Gyr
$^{234}\text{Th}_{90}$	24.10 d
$^{234}\text{Pa}_{91}$	1.17 m
$^{234}\text{U}_{92}$	245.5 kyr
$^{230}\text{Th}_{90}$	75.38 kyr
$^{226}\text{Ra}_{88}$	1600 y
$^{222}\text{Rn}_{86}$	3.8235 d
$^{218}\text{Po}_{84}$	3.10 m
$^{214}\text{Pb}_{82}$	26.8 m
$^{214}\text{Bi}_{83}$	19.9 m
$^{214}\text{Po}_{84}$	164.3 μs
$^{210}\text{Pb}_{82}$	22.3 y
$^{210}\text{Bi}_{83}$	5.013 d
$^{210}\text{Po}_{84}$	138.376 d
$^{206}\text{Pb}_{82}$	$> 10^{20}$ yr

actinium series

$^{235}\text{U}_{92}$	0.7038 Gyr
$^{231}\text{Th}_{90}$	25.52 h
$^{231}\text{Pa}_{91}$	32760 y
$^{227}\text{Ac}_{89}$	21.773 y
$^{227}\text{Th}_{90}$	18.72 d
$^{223}\text{Ra}_{88}$	11.435 d
$^{219}\text{Rn}_{86}$	3.96 s
$^{215}\text{Po}_{84}$	1.781 ms
$^{211}\text{Pb}_{82}$	36.1 m
$^{211}\text{Bi}_{83}$	2.14 m
$^{207}\text{Tl}_{81}$	4.77 m
$^{207}\text{Pb}_{82}$	$> 10^{20}$ yr

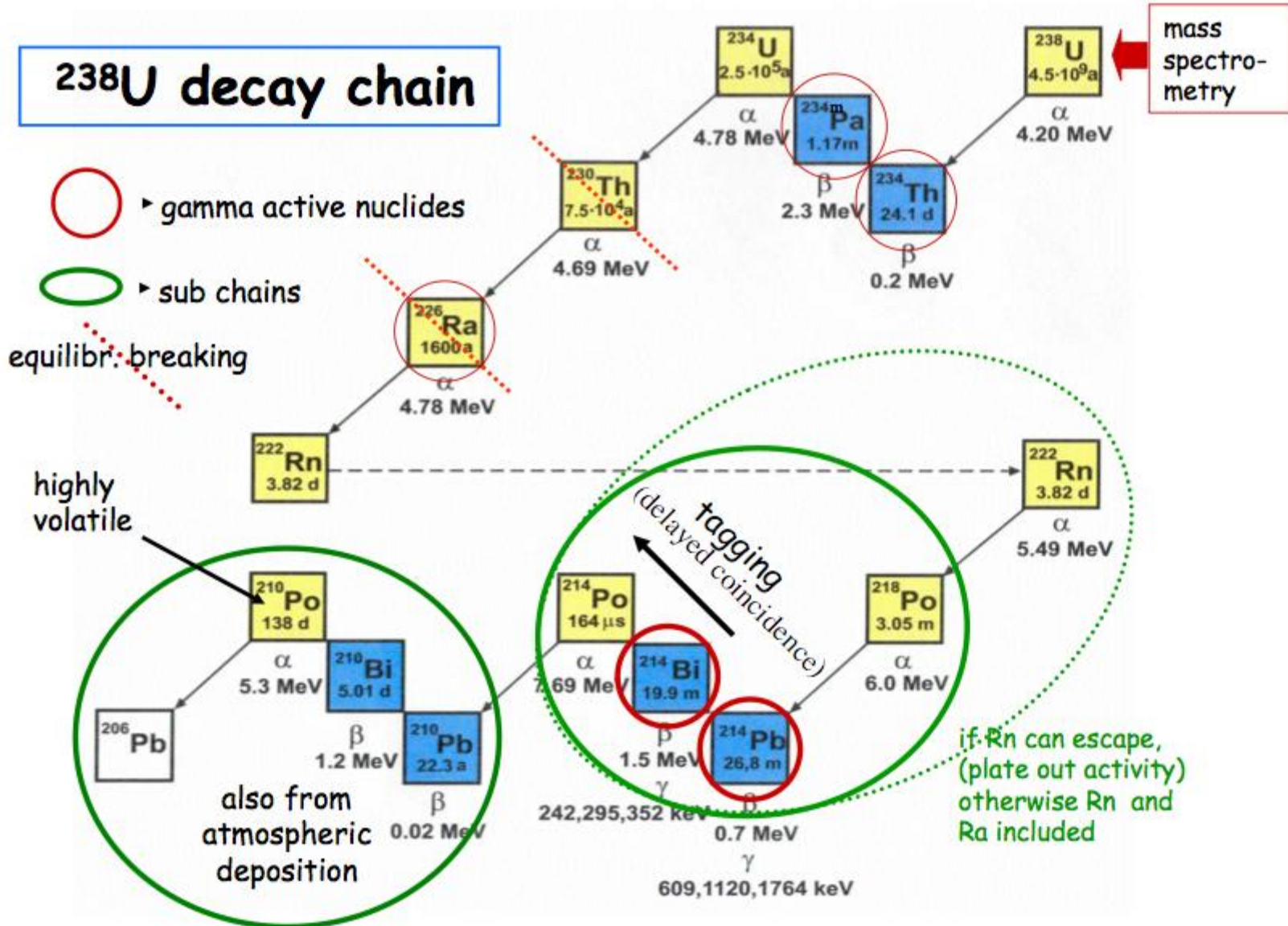
thorium series

$^{232}\text{Th}_{90}$	14.05 Gyr
$^{228}\text{Ra}_{88}$	5.75 y
$^{228}\text{Ac}_{89}$	6.15 h
$^{228}\text{Th}_{90}$	1.9116 y
$^{224}\text{Ra}_{88}$	3.66 d
$^{220}\text{Rn}_{86}$	55.6 s
$^{216}\text{Po}_{84}$	0.145 s
$^{212}\text{Pb}_{82}$	10.64 h
$^{212}\text{Bi}_{83}$	60.55 m
64% $^{212}\text{Po}_{84}$	0.299 μs
36% $^{208}\text{Tl}_{81}$	3.053 m
$^{208}\text{Pb}_{82}$	$> 10^{20}$ yr

disequilibrium in natural decay chains

sample	activity of U/Th progenies [mBq/kg] and their ratios					
	$^{234\text{m}}\text{Pa}$	^{226}Ra	$^{234\text{m}}\text{Pa}/^{226}\text{Ra}$	^{228}Th	^{228}Ra	$^{228}\text{Th}/^{228}\text{Ra}$
WTS steel	121 \pm 18	0.99 \pm 0.15	122 \pm 26	3.7 \pm 0.4	1.7 \pm 0.2	2.18 \pm 0.35
pre WW1 steel	5.7 \pm 1.4	0.15 \pm 0.02	38 \pm 11	0.46 \pm 0.07	0.47 \pm 0.05	0.98 \pm 0.18

^{238}U decay chain



Origin of radioactive contaminations

Fossil radioactivity (present since the formation on the Earth)

- Most elements present on Earth condensed from a interstellar cloud about 4.5×10^9 yr ago.
- This cloud consisted (mostly) of “primordial” ^1H and ^4He produced in the first minutes after the “Big Bang” and heavier elements produced in earlier generations of stars
- At the present epoch, only nuclei with mean lives greater than 10^8 yr are still present in significant numbers

Cosmogenic radioactivity (elements continuously produced by cosmic rays)

Cosmic-rays produce radioactive nuclei via their interactions with nuclei in the atmosphere and in the Earth's crust. \Rightarrow e.g.: the (n,p) reaction on abundant atmospheric nitrogen: $n + ^{14}\text{N} \rightarrow p + ^{14}\text{C}$ $T_{1/2}(^{14}\text{C}) = 5730\text{yr}$

or the “spallation” reactions in a Ge crystal: $n + ^{70}\text{Ge} \rightarrow 3n + ^{68}\text{Ge}$ $T_{1/2}(^{68}\text{Ge}) = 270.7\text{day}$

or for tritium formation in atmosphere: $n + ^{16}\text{O} \rightarrow ^3\text{H} + ^{14}\text{N}$ $T_{1/2}(^3\text{H}) = 12.35\text{yr}$

Artificial radioactivity (due to the development of nuclear technologies)

Most important cosmogenic radionuclides

“Nuclei coinvolti”: the main nuclei in Earth’s crust (atmosphere) involved in the production of the isotopes in the first column

Radio Nuclide	Modo del decadimento	$T_{1/2}$ (anni)	Nuclei coinvolti
3H	β^-	12.33 anni	O,Mg,Si,Fe(O,N)
3He		stabile	(O)
^{10}Be	β^-	$1.51 \cdot 10^6$ anni	O,Mg,Si,Fe(O,N)
^{14}C	β^-	5730 anni	O,Mg,Si,Fe(N)
^{21}Ne		stabile	Mg,Al,Si,Fe
^{36}Cl	β^-	$3.01 \cdot 10^5$ anni	Fe,Ca,K,Cl(Ar)
^{36}Ar	CE, β^+	35 giorni	Fe,Ca,K,Cl(Ar)
^{39}Ar	β^-	269 anni	Fe,Ca,K (Ar)
^{41}Ca	CE; β^+	$1.03 \cdot 10^5$ anni	Ca, Fe
^{129}I	β^-	$1.57 \cdot 10^7$ anni	Te,Ba,La,Ce(Xe)
^{126}Xe		stabile	Te,Ba,La,Ce,I

Origin of radioactive contaminations

Fossil radioactivity (present since the formation on the Earth)

- Most elements present on Earth condensed from a interstellar cloud about 4.5×10^9 yr ago.
- This cloud consisted (mostly) of “primordial” ^1H and ^4He produced in the first minutes after the “Big Bang” and heavier elements produced in earlier generations of stars
- At the present epoch, only nuclei with mean lives greater than 10^8 yr are still present in significant numbers

Cosmogenic radioactivity (elements continuously produced by cosmic rays)

Cosmic-rays produce radioactive nuclei via their interactions with nuclei in the atmosphere and in the Earth's crust. \Rightarrow e.g.: the (n,p) reaction on abundant atmospheric nitrogen: $n + ^{14}\text{N} \rightarrow p + ^{14}\text{C}$ $T_{1/2}(^{14}\text{C}) = 5730\text{yr}$

or the “spallation” reactions in a Ge crystal: $n + ^{70}\text{Ge} \rightarrow 3n + ^{68}\text{Ge}$ $T_{1/2}(^{68}\text{Ge}) = 270.7\text{day}$

or for tritium formation in atmosphere: $n + ^{16}\text{O} \rightarrow ^3\text{H} + ^{14}\text{N}$ $T_{1/2}(^3\text{H}) = 12.35\text{yr}$

Artificial radioactivity (due to the development of nuclear technologies)

Anthropogenic radioactivity

(appeared as result of human activity)

^{60}Co ¹⁾	γ	5.3 y
$^{90}\text{Sr} - ^{90}\text{Y}$ ²⁾	β	29 y
$^{137}\text{Cs}, ^{134}\text{Cs}$ ²⁾	γ	30 y, 2.1 y
$^{238}, ^{239}, ^{240}, ^{242}\text{Pu}$ ³⁾	α	89 y, 24×10^3 y, 6.5×10^3 y, 3.7×10^3 y
$^{241}, ^{243}\text{Am}$ ³⁾	α	432 y, 7370 y
^{244}Cm ³⁾	α	18 y

¹⁾ production of steel

²⁾ nuclear bomb tests; Chernobyl, Fukushima

³⁾ Nuclear power stations; handling of nuclear materials; Chernobyl, Fukushima

Materials radiopurity screening

Material selection is the most fundamental prerequisite in low-radioactivity experiments

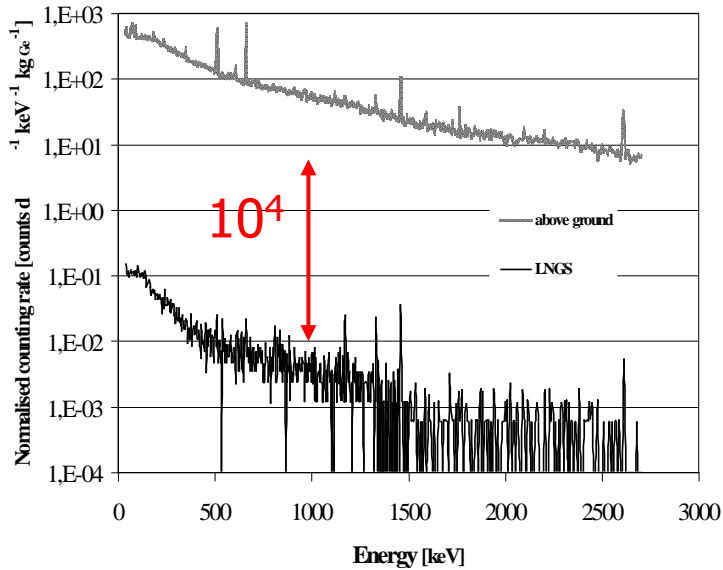
- Chemical methods
- Atomic methods
 - X-ray fluorescence spectrometer: study the characteristic X-rays emission from a sample excited with high-energy X-rays;
 - Atomic absorption spectrometry: study the absorption of optical radiation by atoms of the sample
- Mass-spectrometry
 - The molecules of the sample are firstly ionized, then sorted and separated by external electric and magnetic fields according to their mass-to-charge ratio, and finally detected
- Neutron activation analysis
 - The sample is irradiated with neutrons and unstable isotopes are produced mainly by (n,γ) reactions. They can be identified by γ spectrometry and their concentration determined.
- Gamma spectroscopy
 - The sensitivity can be improved by increase: 1) the sample mass; 2) the measuring time; 3) the detection efficiency
- Especially developed radiopurity test facilities
- The experiment itself as radiopurity detector
 - The detector measures its radioactive contamination itself (active technique). It gives most of the times the best sensitivities

Comparison of different methods sensitivity

method	suited for	sensitivity for U/Th
X-ray fluorescence spectrometry	primordial parents	10 mBq/kg
Alpha spectroscopy	^{210}Po , α emitting nuclides	1 mBq/kg
Liquid scintillation counting	α emitting nuclides	1 mBq/kg
Atom Adsorption Sp.	primordial parents	1-1000 $\mu\text{Bq/kg}$
Mass spectrometry (ICP-MS; GDMS)	primordial parents	1-100 $\mu\text{Bq/kg}$
Ge-spectroscopy*	γ emitting nuclides	10-100 $\mu\text{Bq/kg}$
Scintillation detectors*	internal U/Th	1-10 $\mu\text{Bq/kg}$
Rn emanation assay	^{226}Ra , ^{228}Th	0.1-10 $\mu\text{Bq/kg}$
Neutron activation	primordial parents	0.01 $\mu\text{Bq/kg}$
Large scintillation counters *	U/Th, cosmogenic	1-10 nBq/kg

* Needs counting time of several weeks to several month

Low background STELLA HPGe facility @ LNGS



Low-Level laboratory: 15 HPGe spectrometers

- Material **screening** for experiments
- **Background** characterization
- Development of new **detectors**
- **Physics** measurements (rare decays)
- **Environmental** measurements (radiodating)

GEMPI2 detector: 44 cpd/kg 40-2700 keV

0.13 cpd/kg @ 1460 keV



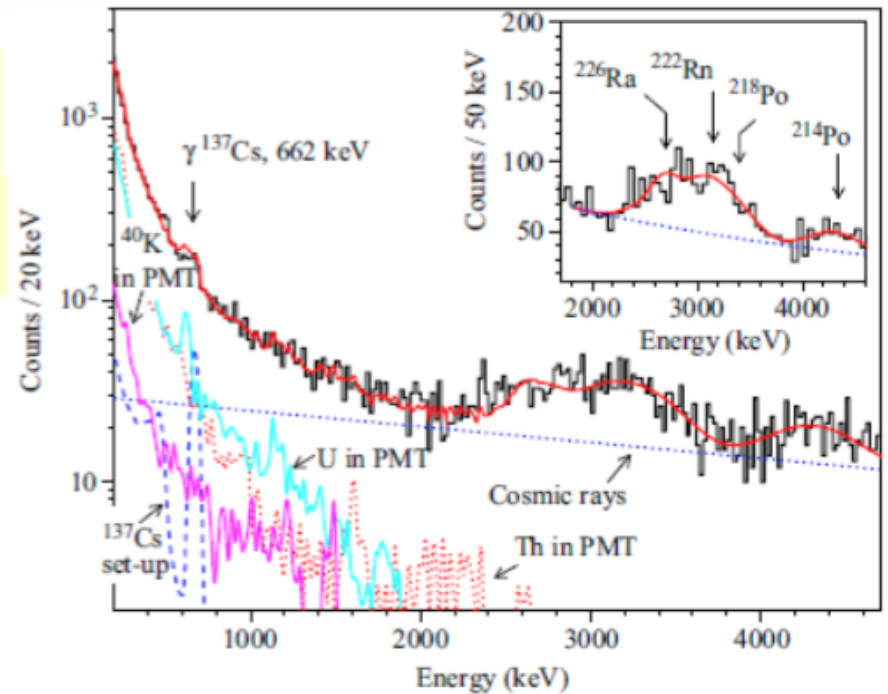
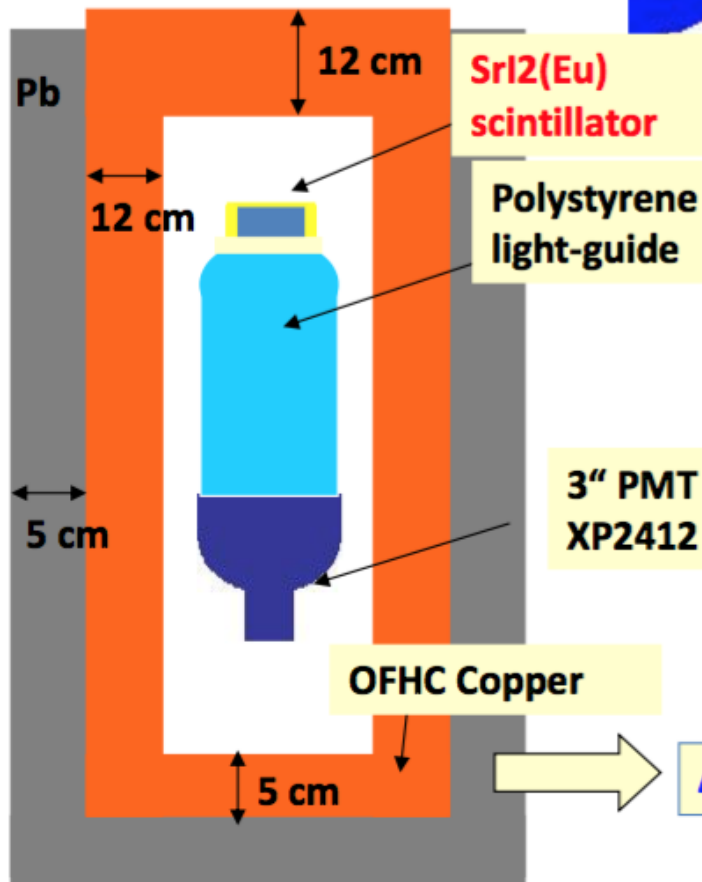
Active method

$\text{SrI}_2(\text{Eu})$ scintillation detector

Plastic scintillator 50×50×10 cm

7" PMT
FEU-125

+ Montecarlo
simulations as a
very useful tool



Purification of the materials

Omnipresence of primordial radionuclides in ores and other raw materials results in a wide range of contamination in the final product

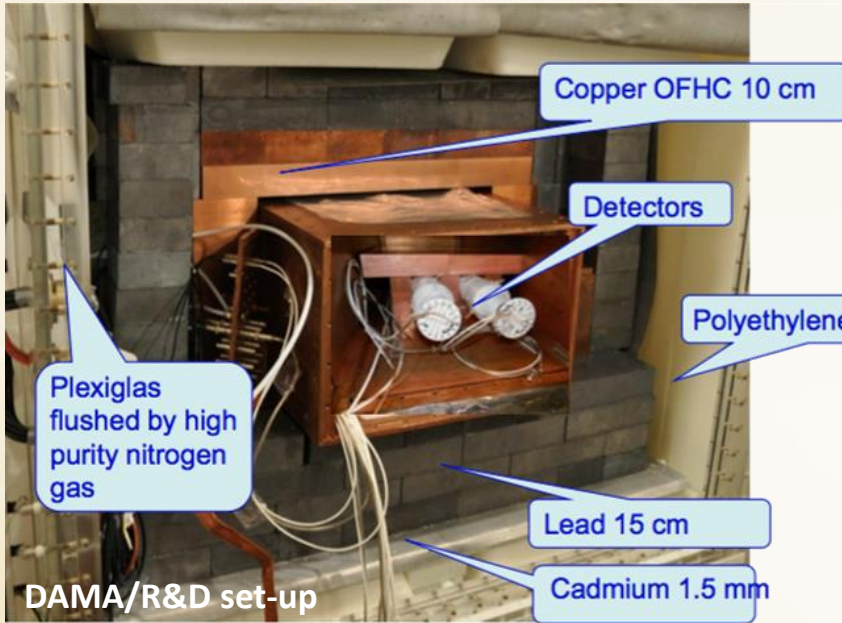
Alongside selection techniques, the purification techniques are equally important

There exist many purification methods that takes advantage of different chemical or physical properties to separate the impurities from the material

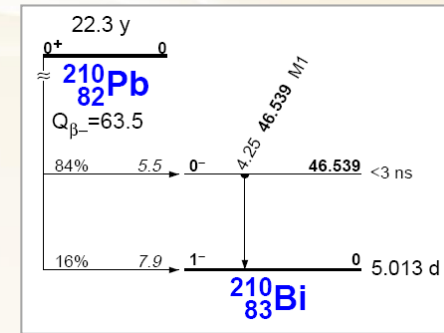
- Crystallization
- Sedimentation
- Filtration
- Distillation
- Sublimation
- Adsorption
- Extraction
- Zone melting
- Chromatography (Ion exchange)
- Electrodialysis
- Reverse osmosis
- Electrophoresis
- Electrolysis
- *Others very specific methods*

Shielding from external background sources

An example of passive shield



A shell-like construction: passive shield typically is made of a few layers to shield against gamma and neutrons, sealing from radon, and to minimize cost



Copper: very radiopure, but more expensive than Lead

Lead: High Z (important to shield γ rays) and low background interference resulting from the interaction with neutrons and μ and from activation. It contains ^{210}Pb ($T_{1/2} = 22 \text{ y}$). Its cost depends on ^{210}Pb concentration

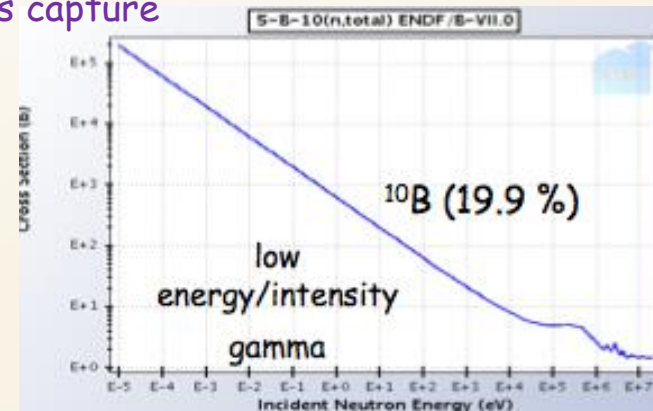
Neutron shield: Polyethylene + Cadmium = moderate + capture

⇒ Low A materials as water, paraffin or polyethylene moderate neutrons

⇒ Materials as Cd, B, Li have an high efficiency for thermal neutrons capture

Three-level system to exclude Radon from the detectors:

- Walls and floor of the installation sealed in Supronyl ($2 \times 10^{-11} \text{ cm}^2/\text{s}$ permeability)
- Whole shield in plexiglas box maintained in HP Nitrogen atmosphere in slight overpressure with respect to environment
- Detectors in the inner Cu box in HP Nitrogen atmosphere in slight overpressure with respect to environment



A curiosity: the use of Roman lead

Navis oneraria magna

- Sank ~70 a.c. at ~7 miles from the Sardinian coast (Oristano) at 28 m depth
- 2000 Lead bricks of 33 kg each, ~1000 recovered
- Absence of X-rays and bremsstrahlung from 1162 keV β decay

Roman lead is used in fundamental physics and in Industry (low activity soldering)

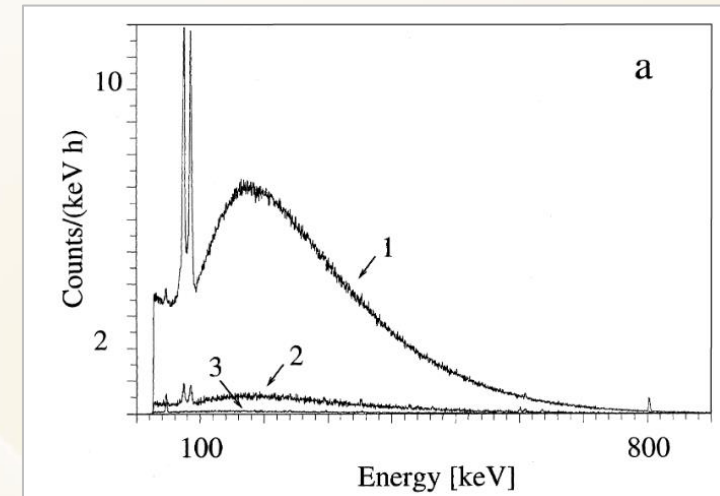
Measurement of lead with GeMPI

lead sample	weight [kg]	time [d]	specific activity [$\mu\text{Bq/kg}$]				
			^{226}Ra	^{228}Th	^{40}K	^{207}Bi	^{210}Pb
DowRun	144.6	101.7	< 29	< 22	440 ± 140	98 ± 24	$(2.7 \pm 0.4) \times 10^7$
Boliden	144.3	75.0	< 46	< 31	460 ± 170	< 13	$(2.3 \pm 0.4) \times 10^7$
roman	22.1	37.2	< 45	< 72	< 270	< 19	< 1.3×10^6
bolometric measurement: Allesandrello et al. NIM B142 (1998) 163							< 4×10^3

^{210}Pb is ~200 Bq/kg in common lead

Spectra recorded with shields made with various types of lead.

1. Common modern lead;
2. Modern lead with a certified content of less than 20 Bq/kg of ^{210}Pb
3. Roman lead from Oristano

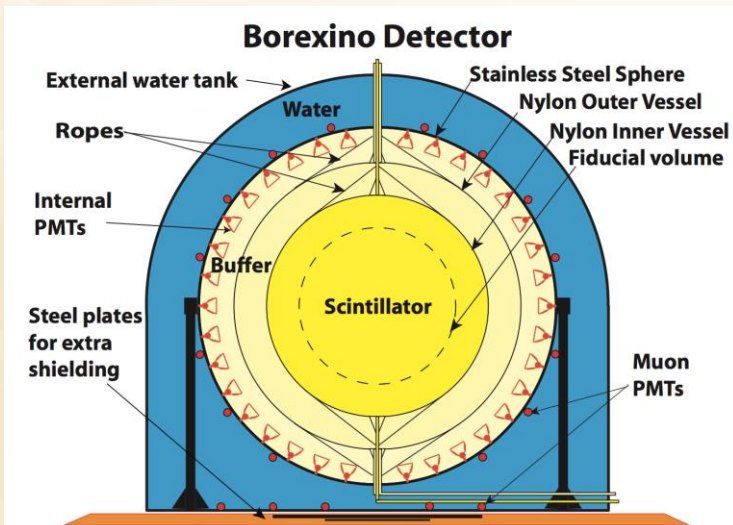


Shielding from external background sources

Examples of active shield (VETO)

The external layer of the detector serves as an active shield (e.g. for cosmic muons veto):

- Outer water Cherenkov detector;
- Plastic scintillators
- Liquid Scintillators
- Inorganic scintillators

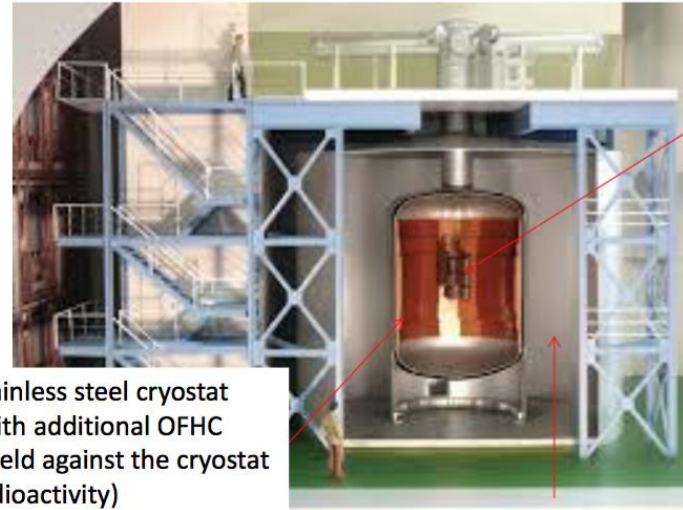


Water can be deeply purified by complex approach (e.g. in Borexino):

- filtering (0.1 μm)
- Osmosis unit
- De-ionization
- Current flow of high purity nitrogen in a stripping column

Water is unavoidable for very large set-ups due to high cost of metals

GERDA water shield



Stainless steel cryostat
(with additional OFHC
shield against the cryostat
radioactivity)

Ultra-pure water passive
shield, acts also as active
Cherenkov muon veto

Bare HPGe detectors ^{76}Ge

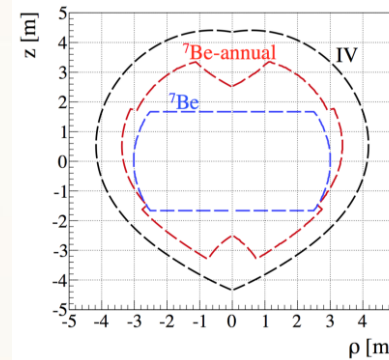
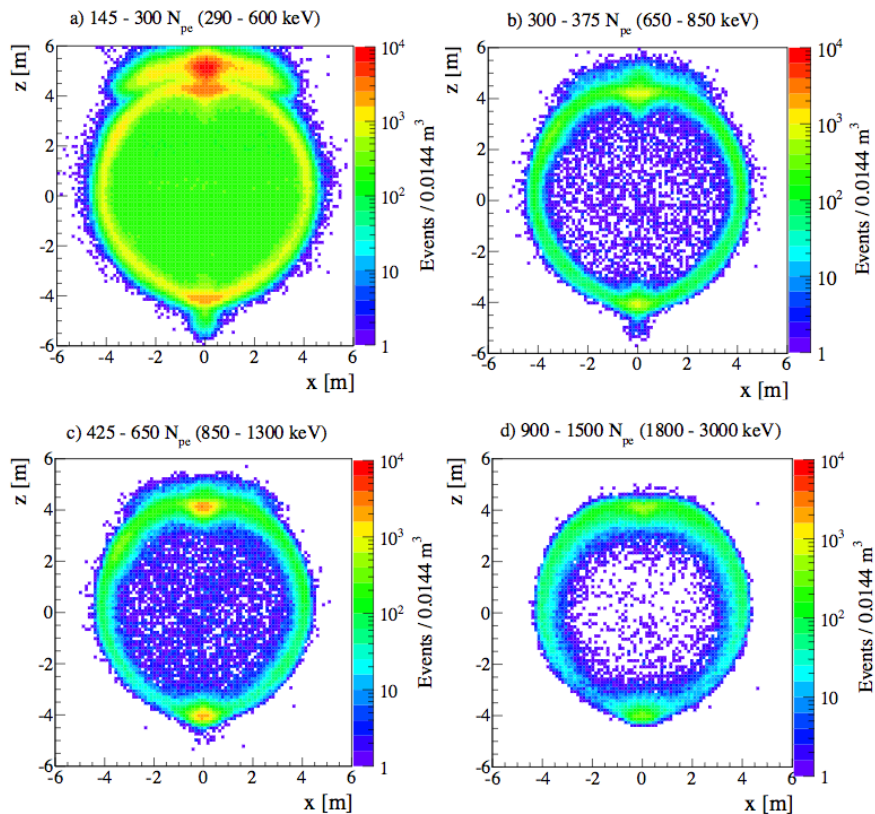
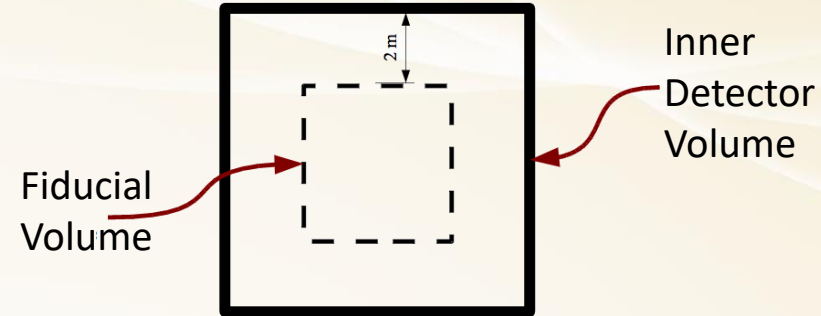


Shielding from external background sources

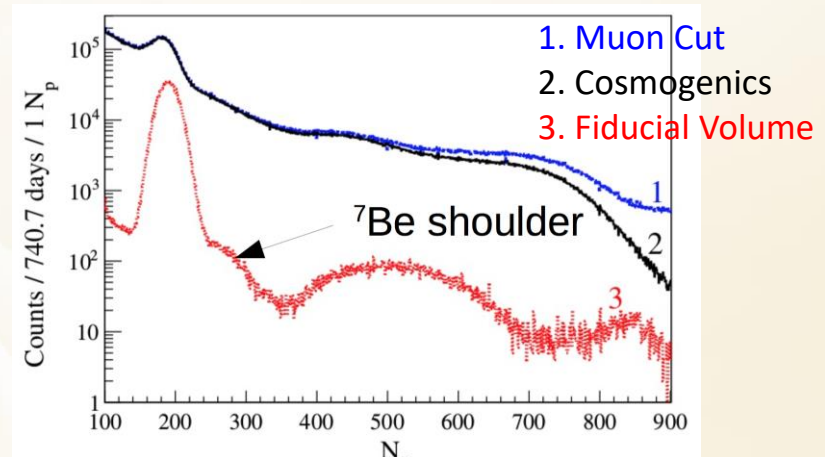
Use of Fiducial Volume

The volume where the background is reduced that will be used to make physics measurements

- The choice of the FV is related to the effect searched for
- Trade off between high exposure and low background



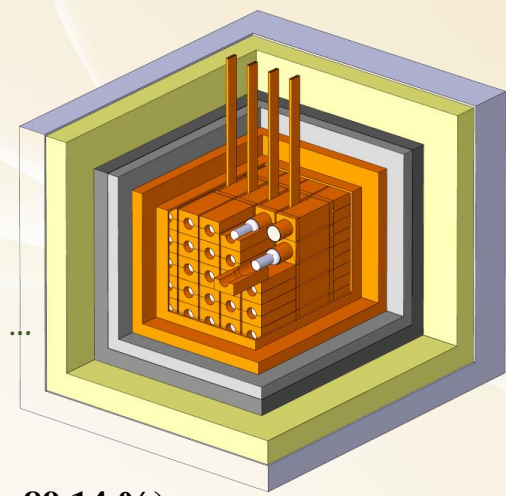
The case of Borexino



Techniques for Background identification

Coincidence technique

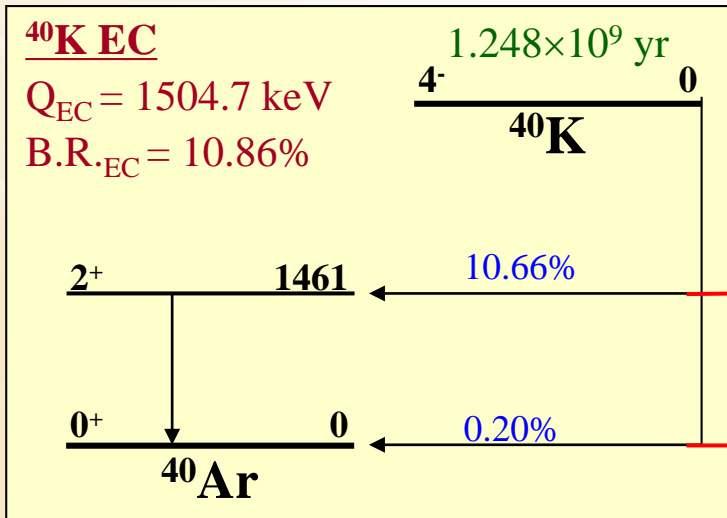
In set-up with many detectors the anti-coincidence technique can strongly reduce background. Its effectiveness depends on many factors as, e.g., set-up geometry, energy threshold, presence of passive materials between detectors, ...



An example from DAMA/LIBRA exp. (matrix 5x5 NaI(Tl) detectors)

residual ^{nat}K

^{40}K : $\delta = 0.0117\%$; $T_{1/2} = 1.248 \times 10^9 \text{ yr}$ (EC = 10.86%; $\beta^- = 89.14\%$)

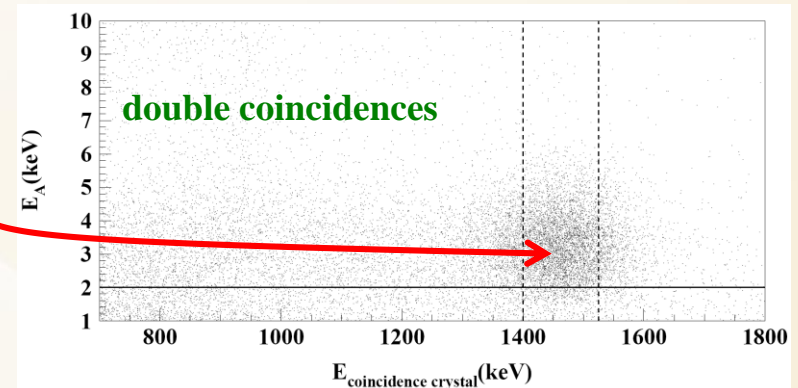
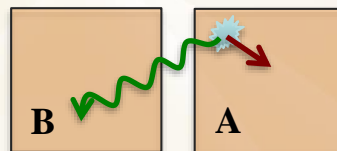


The probability for ^{40}K EC from shell K to the 1461 keV level of ^{40}Ar is: $P_{^{40}\text{K} \text{ EC} \rightarrow 1461} = 10.66\% \times 76.3\% = 8.1\%$ in such a case a 1461 keV γ is emitted together with the 3.2 keV X-rays/Auger electrons from shell K of ^{40}Ar (this last is contained in the detector with efficiency ~ 1)

L1461: $\text{EC}_K = 76.3\%$; $\text{EC}_L = 20.9\%$; $\text{EC}_{M+} = 2.74\%$

L0: $\text{EC}_K = 87.9\%$; $\text{EC}_L = 8.6\%$; $\text{EC}_{M+} = 1.26\%$

The 1461 keV γ can escape from one detector (A) and hit another one causing a double coincidence. X-rays/Auger electrons give rise in A to a 3.2 keV peak



Techniques for Background identification

Pulse Shape Discrimination (PSD)

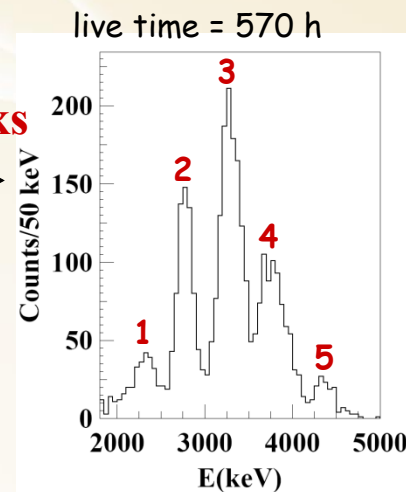
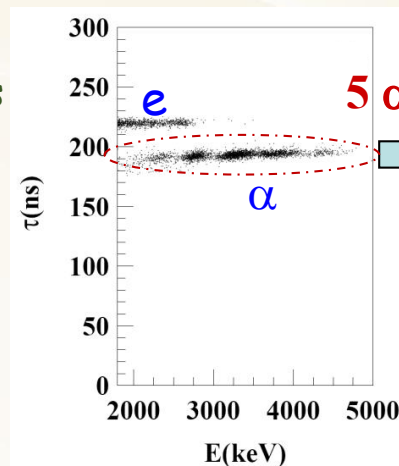
the study of the shape of scintillation pulses can be used to identify events induced by different particles

An example:

Identification of α particles from ^{238}U and ^{232}Th residual contamination in a NaI(Tl) of DAMA/LIBRA

α/e PSD has practically 100% effectiveness in NaI(Tl)

$$\tau = \frac{\int t \cdot f(t) dt}{\int f(t) dt} \approx \frac{\sum_i h_i t_i}{\sum_i h_i}$$



Contributions of α decays from ^{232}Th and ^{238}U chains to the five measured peaks

1. $^{232}\text{Th}(Q_\alpha=4.08 \text{ MeV}) + ^{238}\text{U}(4.27 \text{ MeV})$
2. $^{234}\text{U}(4.86 \text{ MeV}) + ^{230}\text{Th}(4.77 \text{ MeV}) + ^{226}\text{Ra}(4.87 \text{ MeV})$
3. $^{210}\text{Po}(5.41 \text{ MeV}) + ^{228}\text{Th}(5.52 \text{ MeV}) + ^{222}\text{Rn}(5.59 \text{ MeV}) + ^{224}\text{Ra}(5.79 \text{ MeV})$
4. $^{218}\text{Po}(6.12 \text{ MeV}) + ^{212}\text{Bi}(6.21 \text{ MeV}) + ^{220}\text{Rn}(6.41 \text{ MeV})$
5. $^{216}\text{Po}(6.91 \text{ MeV})$

The study of the α particles energy distributions exclude that ^{238}U decay chain is at equilibrium

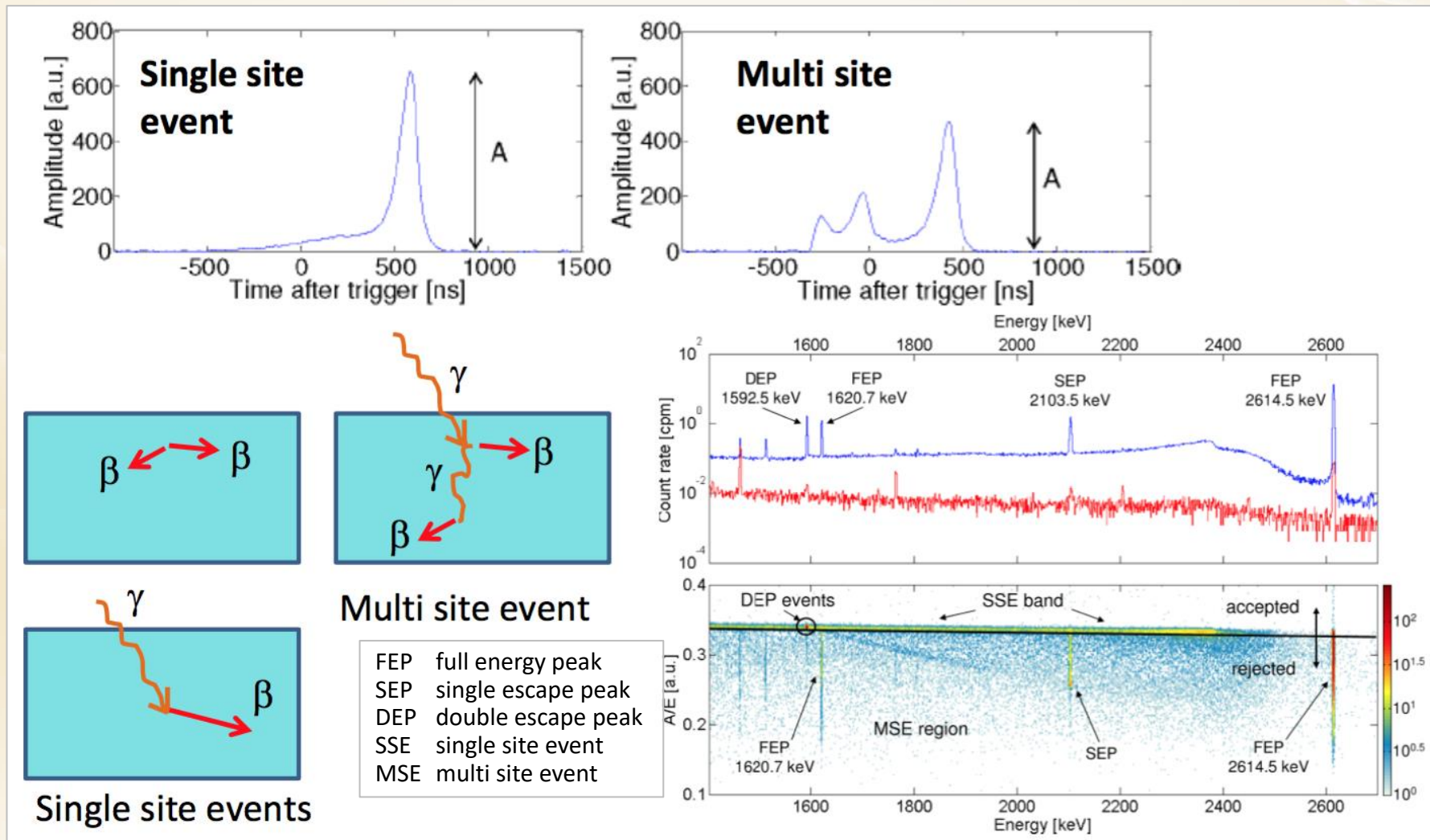
^{238}U chain split into 5 subchains: $^{238}\text{U} \rightarrow ^{234}\text{U} \rightarrow ^{230}\text{Th} \rightarrow ^{226}\text{Ra} \rightarrow ^{210}\text{Pb} \rightarrow ^{206}\text{Pb}$



- (2.1 ± 0.1) ppt of ^{232}Th ;
- (0.35 ± 0.06) ppt for ^{238}U
- (15.8 ± 1.6) $\mu\text{Bq/kg}$ for $^{234}\text{U} + ^{230}\text{Th}$ subchain
- (21.7 ± 1.1) $\mu\text{Bq/kg}$ for ^{226}Ra subchain
- (24.2 ± 1.6) $\mu\text{Bq/kg}$ for ^{210}Pb subchain

Techniques for Background identification

Pulse Shape Discrimination between single site events and multi site events in HPGe detectors (very useful, e.g., in double beta decay searches)



Techniques for Background identification

Time-Amplitude Analysis

Study of correlated events in time: the arrival time and energy of each event is used for selection of fast decay chains in ^{232}Th , ^{238}U or ^{235}U family

Example for ^{232}Th case in DAMA/LIBRA exp.

The searched decay sequence in ^{232}Th family:

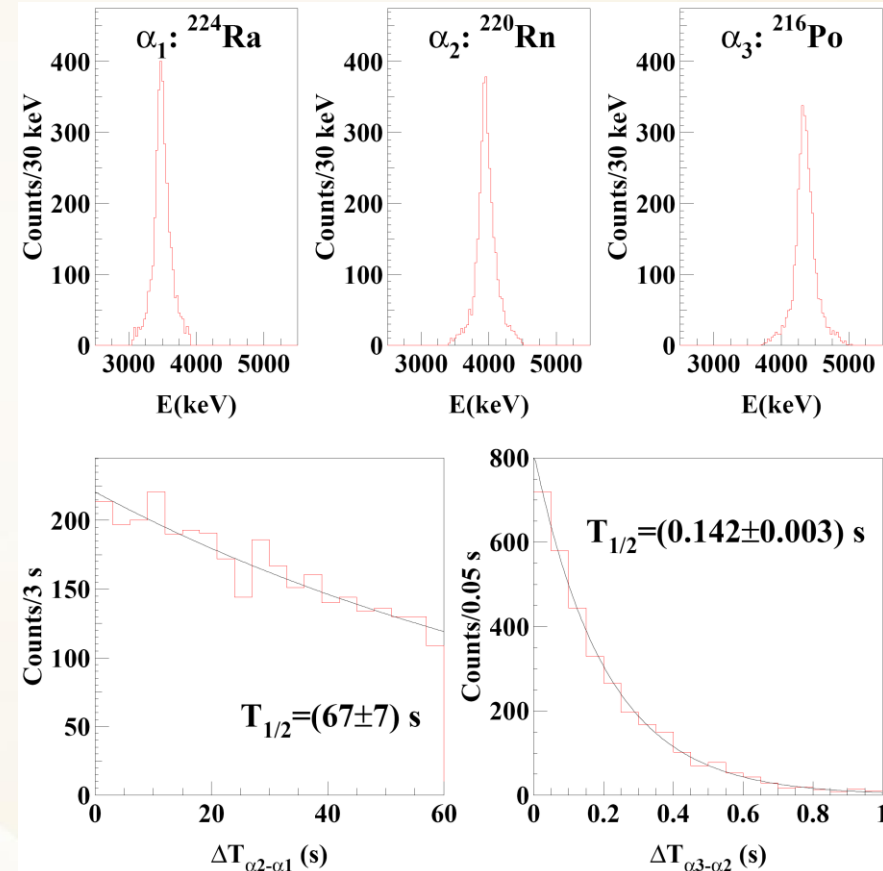
- ^{224}Ra ($Q_\alpha=5.8$ MeV, $T_{1/2}=3.66$ d)
- ^{220}Rn ($Q_\alpha=6.4$ MeV, $T_{1/2}=55.6$ s)
- ^{216}Po ($Q_\alpha=6.9$ MeV, $T_{1/2}=0.145$ s)
- ^{212}Pb

This sub-chain has been selected by looking for:

1. events in the energy window 3050-3900 keV
2. followed within 60 s
3. by another event in the energy window 3400-4500 keV
4. still followed within 1 s
5. by the last event in the energy window 3650-5100 keV

$$\alpha / \beta = 0.467(6) + 0.0257(10) \times E_\alpha [\text{MeV}]$$

α peaks as well as the distributions of the time intervals between the events are in a good agreement with those expected



3310 triple delayed coincidences in 8100 kg×day
 → (9.0 ± 0.4) $\mu\text{Bq/kg}$

Which detectors are used in the search for rare processes

It depends on the searched process.

Some features are common to most experiments as, e.g., high radio-purity levels and large target mass. Others are specific of the searched process as, e.g., high energy resolution and large number of candidate isotopes for $0\nu\beta\beta$ decay searches, or low energy threshold for Dark Matter experiments

- Scintillation detectors
- Cherenkov counters
- Semiconductor detectors
- Cryogenic bolometers
- Geiger, proportional counters (radiochemical experiments)
- Time projection chambers
- Two-phase time projection chambers
- Bubble chambers (Picasso)
- Track foils, emulsions
- Neutron detection
- ...

Characteristics of detectors

- Energy
 - Time
 - Coordinate
 - Dead time
 - Density, Z_{eff} (detection efficiency)
 - Composition (presence of certain elements)
 - Available volume
 - Radiopurity
 - Operational stability
- } resolution

Which detectors are used in the search for rare processes

- There is no "ideal" detector, a variety of detectors is used in astroparticle physics
- Advantage of scintillation detectors: presence of element of interest, stability, good spectrometric and time properties, large volume (liquid scintillators), very radiopure.
- Semiconductor detectors and bolometers provide a very high energy resolution
- Cherenkov detectors used in a case of huge mass request, allow to measure direction of particles, can use water (ice, air) as detector material
- Sometimes a combination of different detectors is used in astroparticle-physics experiments

DIRECT DARK MATTER DETECTION

DAMA/LIBRA (NaI) ★
 KIMS (CsI)
 XMASS (Xe)
 ANAIS (NaI)
 DM-Ice (NaI)
 DEAP3600 (Ar)
 MinicLEAN (Ar)

XENON100 (Xe)
 ZEPLIN-III (Xe)
 LUX (Xe)
 XENON1T (Xe)
 ArDM (Ar)
 DarkSide (Ar)

Superheated
 liquids
 (bubble)

PICASSO (C₄F₁₀)
 SIMPLE (C₂ClF₅)
 COUPP (CF₃I)

Scintillation
 (light)

Phonon
 (heat)

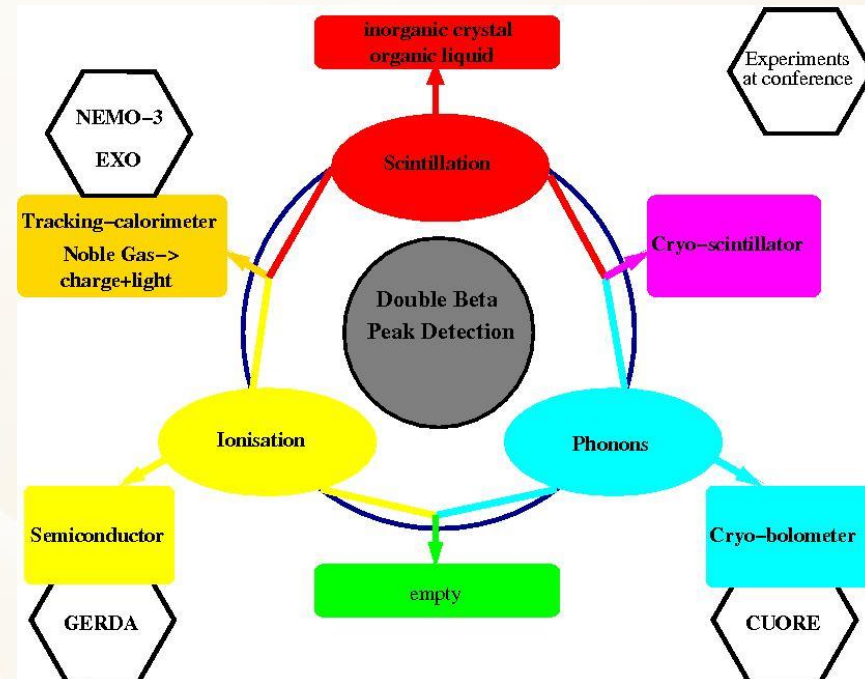
Ionization
 (charge)

CoGeNT (Ge) ★
 TEXONO-CDEX (Ge)
 C-4 (Ge)
 DRIFT (CS₂)
 DM-TPC (CF₄)
 NEWAGE (CF₄)
 MIMAC (³He/CF₄)
 MAJORANA (Ge)
 GERDA (Ge)

CDMS (Ge, Si) ★
 EDELWEISS-II (Ge)
 SuperCDMS (Ge)
 EURECA (Ge)

CRESST (CaWO₄) ★
 EURECA (CaWO₄)

CUORE (TeO₂)

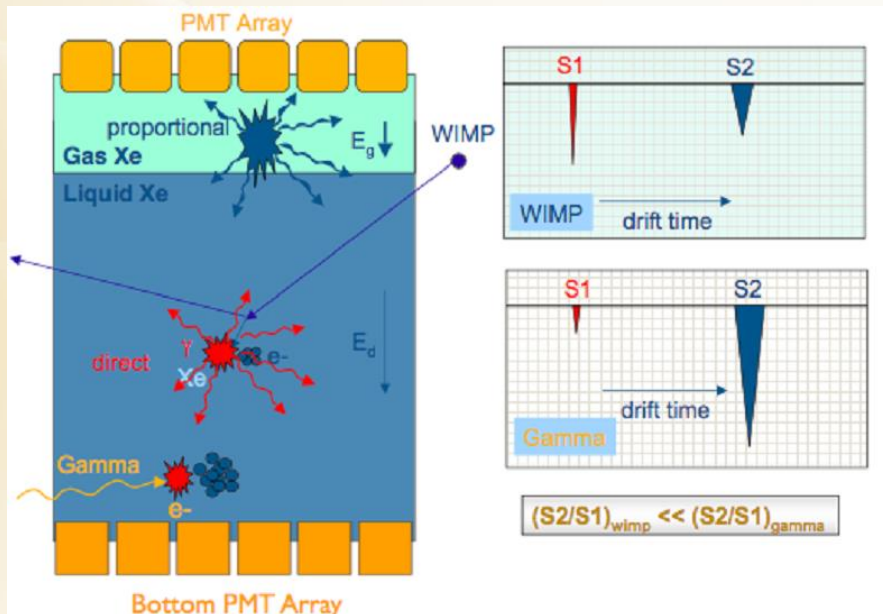


Examples of combined detectors

To achieve a statistical discrimination of different kinds of particles

Dual phase TPC detectors:

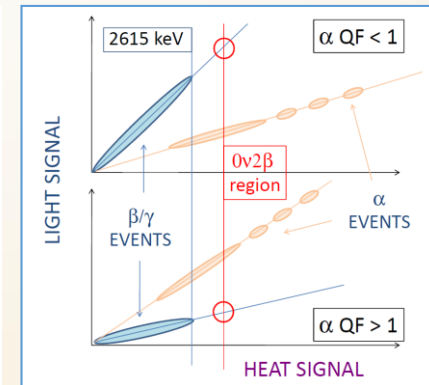
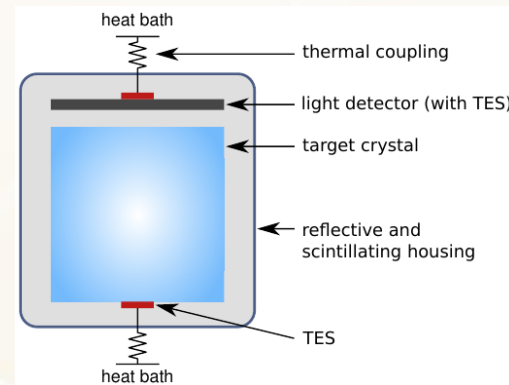
- prompt signal (S1): UV photons from excitation and ionization
- delayed signal (S2): e^- drifted into gas phase and secondary scintillation due to ionization in electric field



XENON, WARP, Dark Side, LUX

Scintillating bolometers:

- Energy deposited in the bolometer via a particle interaction is visible as a heat signal
- A small amount of the energy deposited is emitted as scintillation light collected by a light detector
- Discrimination between α particles, e^- or nuclear recoils can be achieved using as discrimination parameter the fraction of light and heat energy



CRESST, LUCIFER, LUMINEU, AMoRE

Experimental approaches to $\beta\beta$ decay direct searches

Experiment observes $N^{0\nu} = \ln 2 \frac{N_A}{A} \cdot a \cdot \epsilon \cdot Mt / T_{1/2}$ and $N^{bkg} = Mt \cdot B \cdot \Delta E$

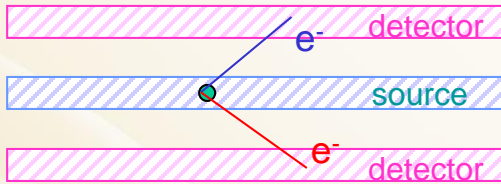
Experimental sensitivity

$$T_{1/2}(90\%CL) > \begin{cases} \frac{\ln 2}{2.3} \frac{N_A}{A} a \cdot \epsilon \cdot Mt & \text{for } N^{bkg} = 0 \\ \frac{\ln 2}{1.64} \frac{N_A}{A} a \cdot \epsilon \sqrt{\frac{Mt}{B \cdot \Delta E}} & \text{for large } N^{bkg} \end{cases}$$

M = mass of detector
t = measurement time
A = isotope mass per mole
 N_A = Avogadro constant
a = fraction of $0\nu\beta\beta$ isotope
 ϵ = detection efficiency
B = background index in units cnt/(keV kg y)
 ΔE = energy resolution = energy window size

①

Source \neq Detector



- scintillation
- gaseous TPC
- gaseous drift chamber with magnetic field and calorimeter

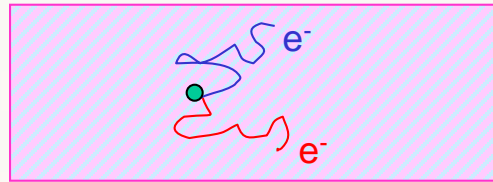
- ☹ difficulties for large source mass
- ☺ neat reconstruction of event topology
- ☺ several candidates with the same detector



Event reconstruction
Low efficiency
Low energy resolution

②

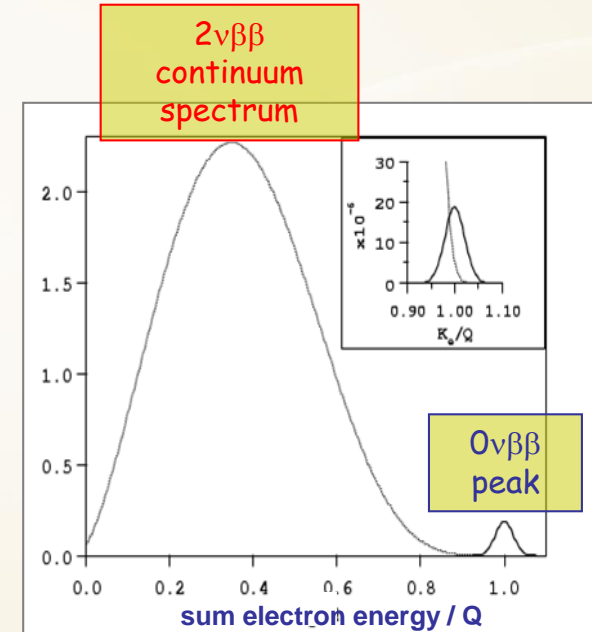
Source \equiv Detector



- scintillation
 - solid-state devices
 - gaseous, liquid detectors
 - cryogenic bolometers
- ☹ constraints on detector materials
 - ☺ very large masses possible
 - ☺ very high energy resolution
 - ☺ Possible indication of event topology



High efficiency
Energy resolution



$Q \sim 2-3$ MeV for the most promising nuclides

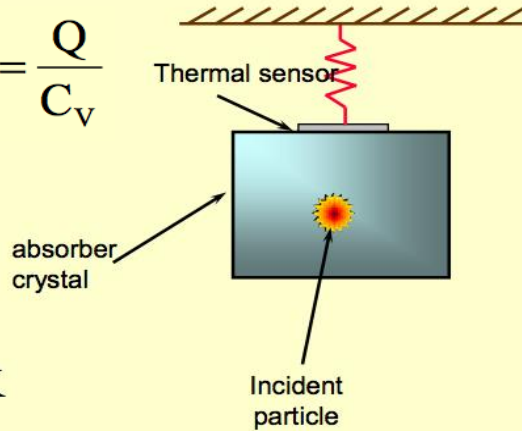


5*1989*1

The cryogenic bolometer

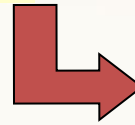


$$\Delta T = \frac{Q}{C_V}$$



- ◆ Temperature signal: $\Delta T = E/C \cong 0.1 \text{ mK}$ for $E = 1 \text{ MeV}$
- ◆ Bias: $I \cong 0.1 \text{ nA} \Rightarrow$ Joule power $\cong 1 \text{ pW}$
 \Rightarrow Temperature rise $\cong 0.25 \text{ mK}$
- ◆ Voltage signal: $\Delta V = I \times dR/dT \times \Delta T$
 $\Rightarrow \Delta V = 1 \text{ mV}$ for $E = 1 \text{ MeV}$
- ◆ Signal recovery time: $\tau = C/G \cong 0.5 \text{ s}$
- ◆ Noise over signal bandwidth (a few Hz): $V_{\text{rms}} = 0.2 \text{ } \mu\text{V}$

$$C_V = 1944 \frac{V}{V_m} \left(\frac{T}{\Theta}\right)^3 \text{ J/K}$$

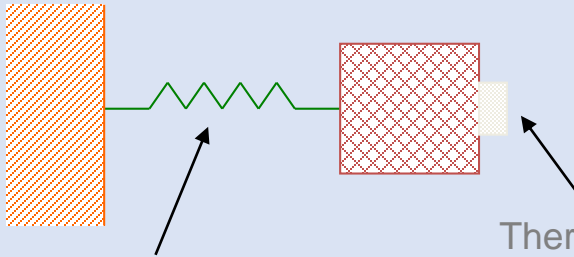


Energy resolution (FWHM): $\cong \text{keV scale}$

Heat sink
 $T \cong 10 \text{ mK}$

Energy absorber
 TeO_2 crystal

$C \cong 2 \text{ nJ/K} \cong 1 \text{ MeV} / 0.1 \text{ mK}$

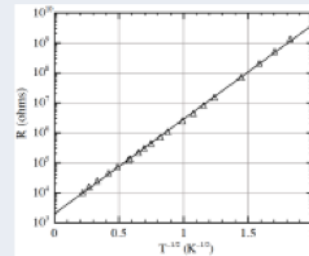


Thermal coupling

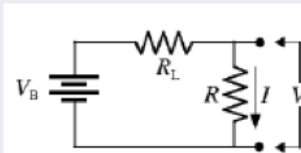
$G \cong 4 \text{ nW / K} = 4 \text{ pW / mK}$

Thermometer
 NTD Ge-thermistor
 $R \cong 100 \text{ M}\Omega$
 $dR/dT \cong 100 \text{ k}\Omega/\mu\text{K}$

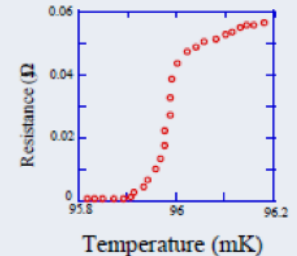
Doped Semiconductors



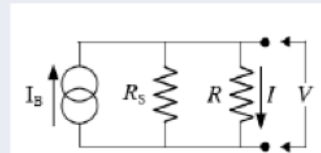
- α negative; $|\alpha| < 10$
- Resistance large
- Current bias and read voltage



Superconducting transition-edge



- α positive; $10 < \alpha < 1000$
- Resistance small
- Voltage bias and read current

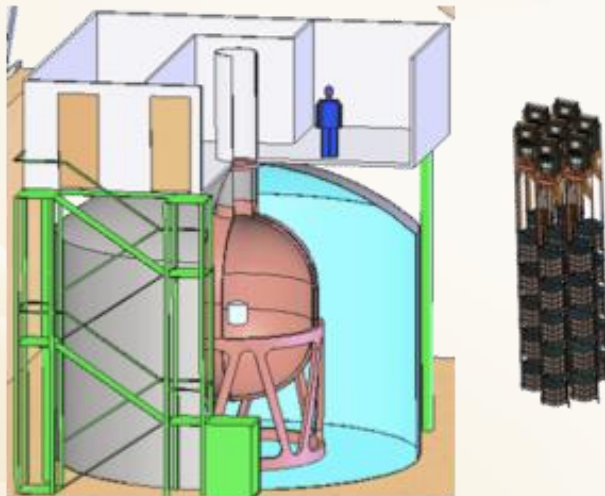




Main LNGS activities on $0\nu\beta\beta$ decay



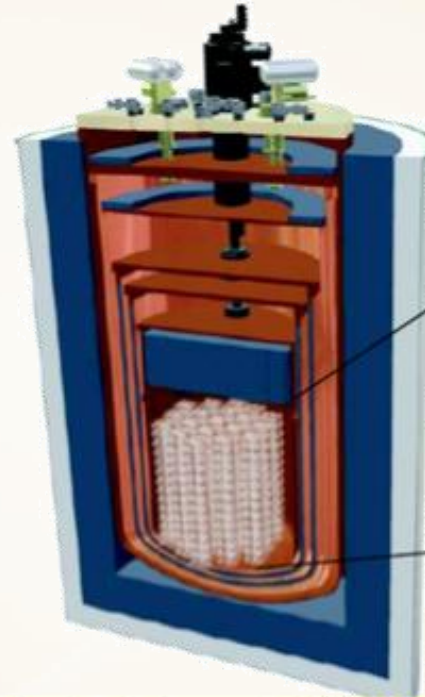
(Germany, Italy, Belgium, Russia)



GERDA

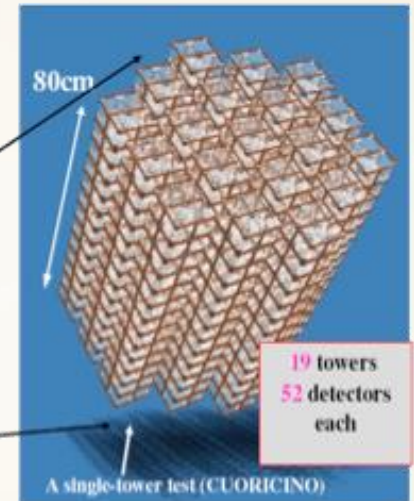
Enriched ^{76}Ge crystals
 Shielding with Liquid N_2 or Ar
 Prove or reject Klapdor's claim,
 then attack inverted hierarchy region

Single dilution refrigerator ~10 mk



for Rare Events

- $\beta\beta_{0\nu}$, Cold Dark Matter, Axion searches
 proposal hep/ph 0501010



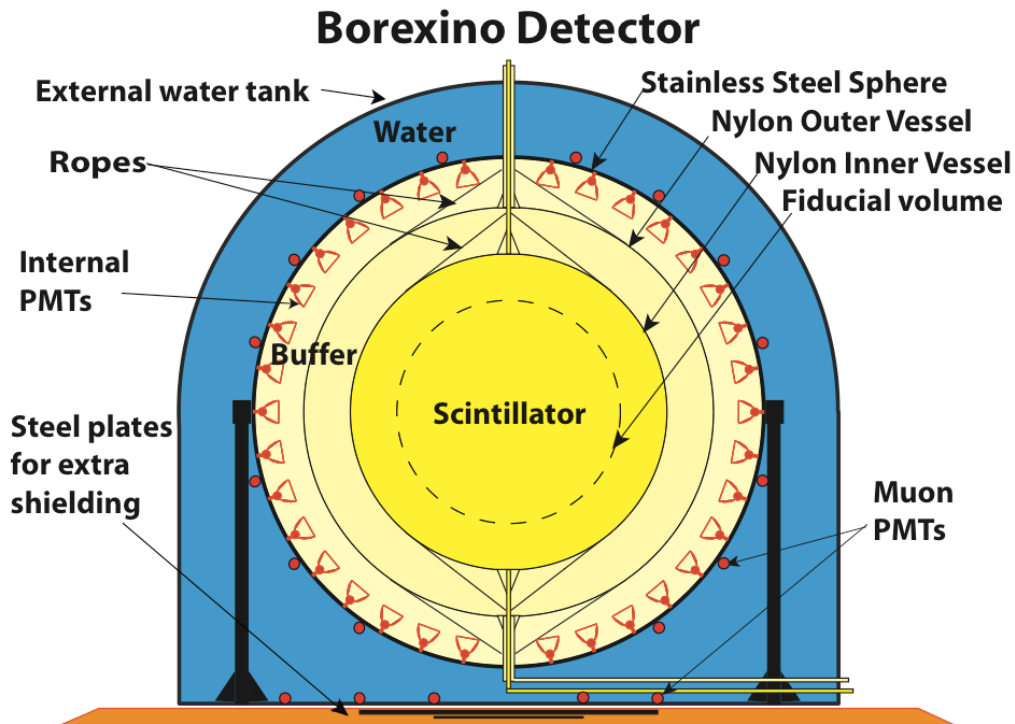
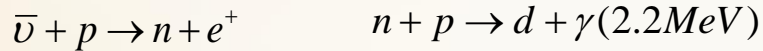
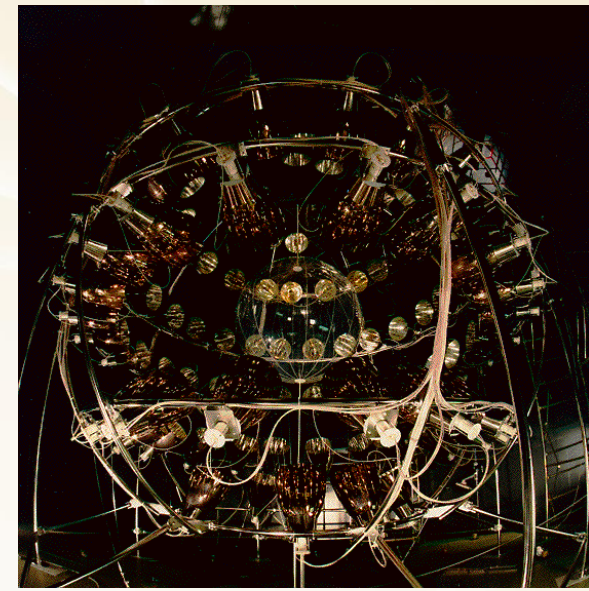
Closed packed array of 988 TeO_2 $5 \times 5 \times 5$ cm^3 crystals $\Rightarrow 741$ kg $\text{TeO}_2 \Rightarrow 204$ kg ^{130}Te

CUORE

TeO_2 crystals. 203 Kg of ^{130}Te
 Goal: 0.01 c/KeV/Kg/y
 m_ν sensitivity $\sim 0.03 - 0.17$ eV

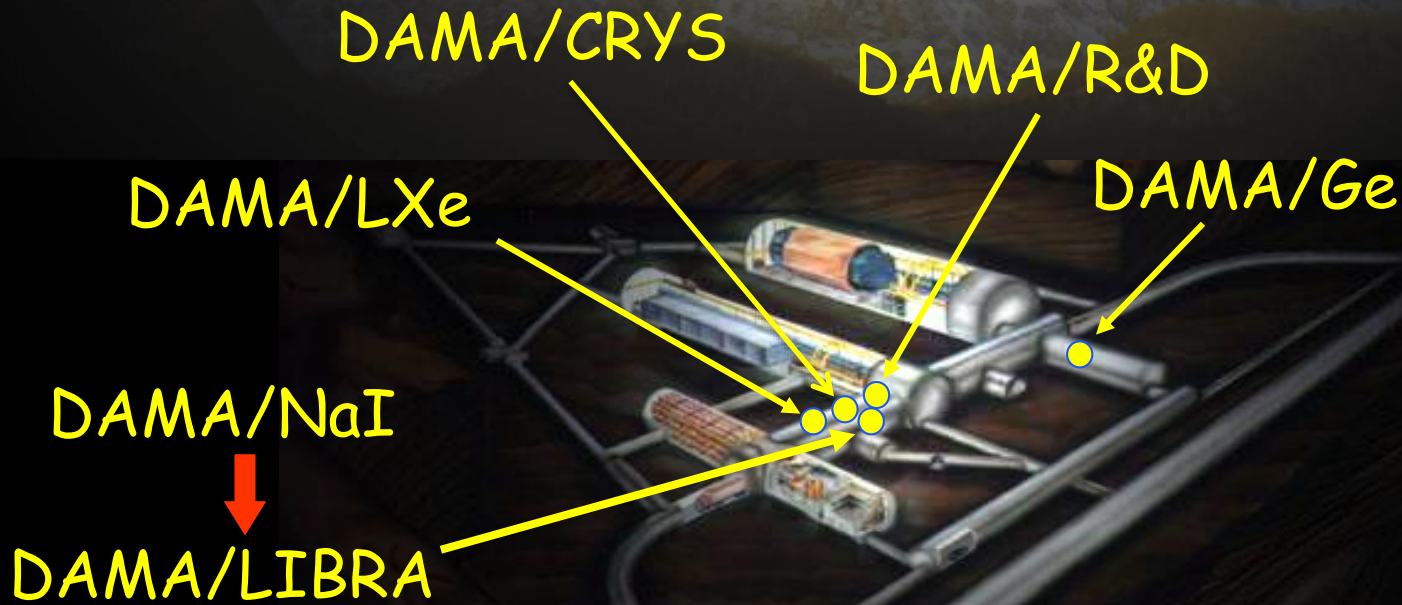
BOREXINO

- Reaction : $\nu_e + e^- \rightarrow \nu_e + e^-$
- Exp. site : Laboratori del Gran Sasso (3300 m.w.e.)
- Target : 300 tons (fid.:100 tons) liquid scintillator
Pseudocumene + PPO, sphere radius 18 m
- Goals : ${}^7\text{Be}$ neutrinos and neutrino spectroscopy.
time behaviour; geo-neutrinos $\bar{\nu}$



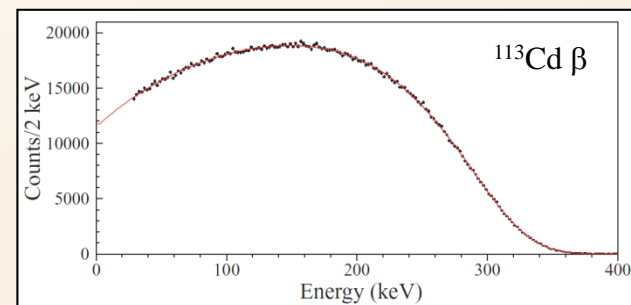
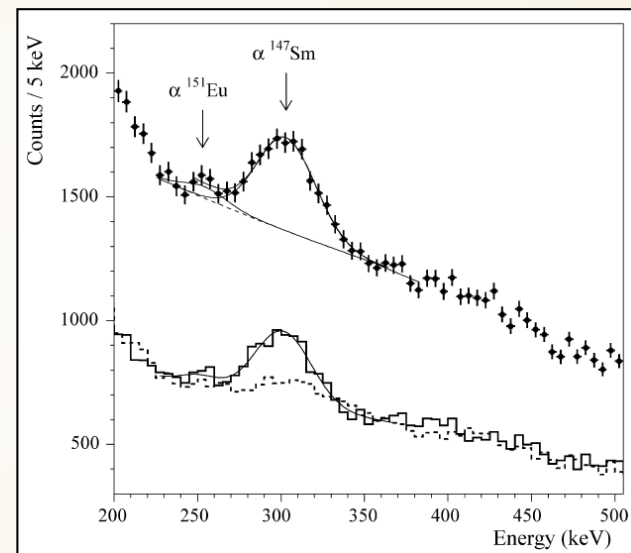
- Borexino
 - Go after ${}^7\text{Be}$ ν 's
 - 300 ton liquid scintillator
 - 2200 8-inch phototubes
 - $E_e > 250$ keV
- Detect $\nu_e + e^- \rightarrow \nu_e + e^-$
 - 55 events/day for SSM

DAMA: an observatory for rare processes @LNGS

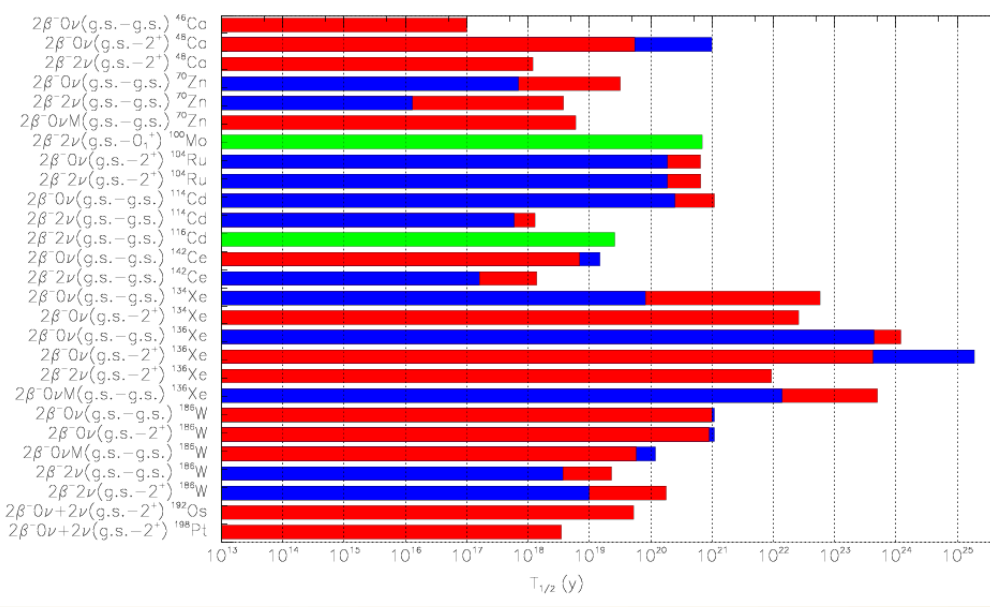
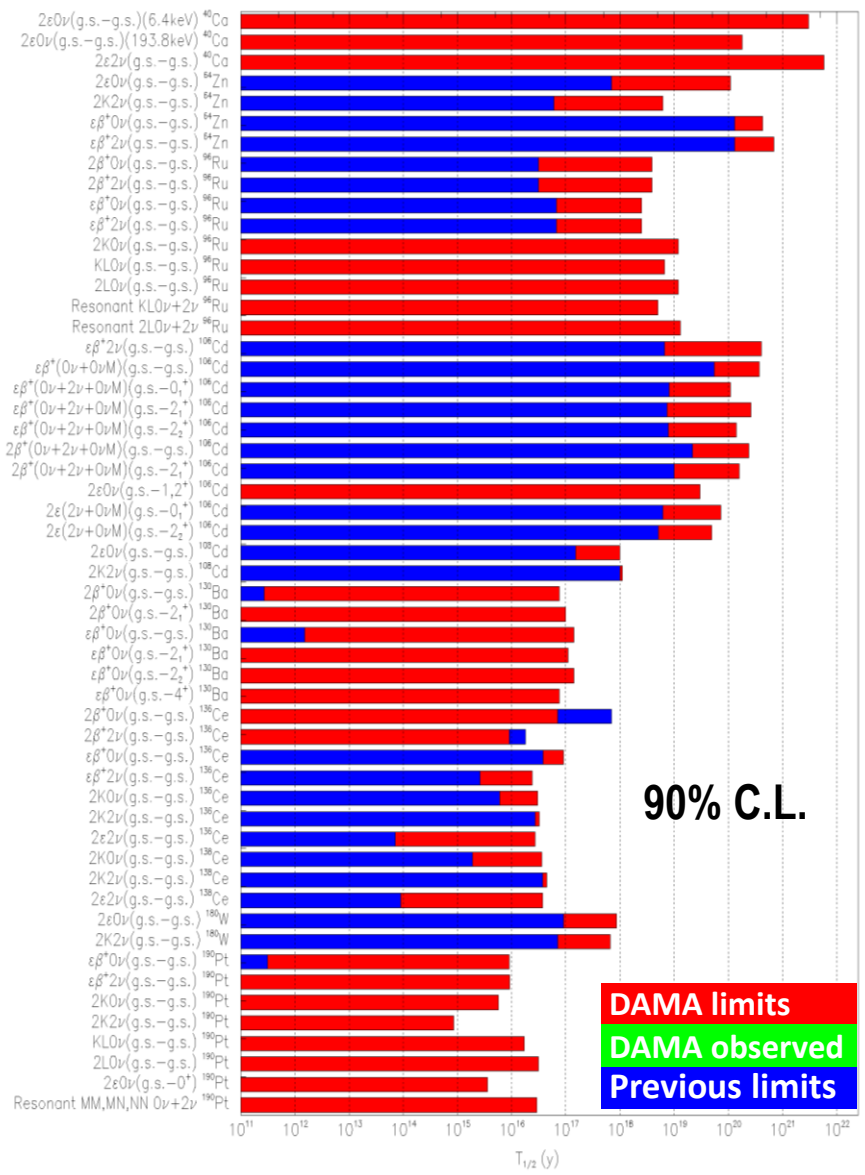


Main recent DAMA results in the search for rare processes

- First or improved results in the search for 2β decays of ~ 30 candidate isotopes: ^{40}Ca , ^{46}Ca , ^{48}Ca , ^{64}Zn , ^{70}Zn , ^{100}Mo , ^{96}Ru , ^{104}Ru , ^{106}Cd , ^{108}Cd , ^{114}Cd , ^{116}Cd , ^{112}Sn , ^{124}Sn , ^{134}Xe , ^{136}Xe , ^{130}Ba , ^{136}Ce , ^{138}Ce , ^{142}Ce , ^{156}Dy , ^{158}Dy , ^{180}W , ^{186}W , ^{184}Os , ^{192}Os , ^{190}Pt and ^{198}Pt
- The best experimental sensitivities in the field for 2β decays with positron emission
- First observation of α decays of ^{151}Eu ($T_{1/2}=5\times 10^{18}\text{yr}$) with a $\text{CaF}_2(\text{Eu})$ scintillator and of ^{190}Pt to the first excited level ($E_{\text{exc}}=137.2\text{ keV}$) of ^{186}Os ($T_{1/2}=3\times 10^{14}\text{yr}$)
- Investigations of rare β decays of ^{113}Cd ($T_{1/2}=8\times 10^{15}\text{yr}$) with CdWO_4 scintillator and of ^{48}Ca with a $\text{CaF}_2(\text{Eu})$ detector
- Observation of correlated e^+e^- pairs emission in α decay of ^{241}Am ($\frac{A_{e^+e^-}}{A_\alpha} \simeq 5 \times 10^{-9}$)
- Search for long-lived super-heavy ekatungsten with radiopure ZnWO_4 crystal scintillator
- Search for CNC processes in ^{127}I , ^{136}Xe , ^{100}Mo and ^{139}La
- Search for ^7Li solar axions resonant absorption in LiF crystal
- Search for spontaneous transition of ^{23}Na and ^{127}I nuclei to superdense state;
- Search for cluster decays of ^{127}I , ^{138}La and ^{139}La
- Search for PEP violating processes in sodium and in iodine
- Search for N, NN, NNN decay into invisible channels in ^{129}Xe and ^{136}Xe



Summary of searches for $\beta\beta$ decay modes in various isotopes (partial list)



ARMONIA: New observation of $2\nu 2\beta^-$ $^{100}\text{Mo} \rightarrow ^{100}\text{Ru}$ (g.s. $\rightarrow 0_1^+$) decay NPA846 (2010)143

AURORA: New observation of $2\nu 2\beta^-$ ^{116}Cd decay J.Phys.:Conf.Ser.718(2016)062009

- Many competitive limits obtained on lifetime of $2\beta^+$, $\epsilon\beta^+$ and 2ϵ processes (^{40}Ca , ^{64}Zn , ^{96}Ru , ^{106}Cd , ^{108}Cd , ^{130}Ba , ^{136}Ce , ^{138}Ce , ^{180}W , ^{190}Pt , ^{184}Os , ^{156}Dy , ^{158}Dy , ...).
- First searches for resonant $0\nu 2\epsilon$ decays in some isotopes

The Dark Side of the Universe: experimental evidences

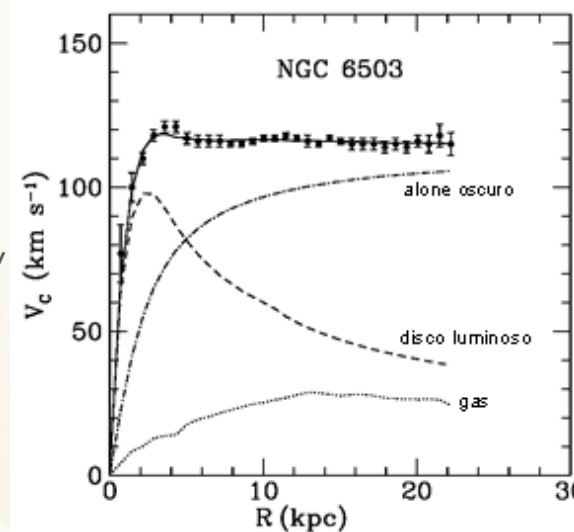


First evidence and confirmations:

- 1933 F. Zwicky: studying dispersion velocity of Coma galaxies
- 1936 S. Smith: studying the Virgo cluster
- 1974 two groups: systematic analysis of *mass density vs distance from centre* in many galaxies

Other experimental evidences

- ✓ from LMC motion around Galaxy
- ✓ from X-ray emitting gases surrounding elliptical galaxies
- ✓ from hot intergalactic plasma velocity distribution in clusters
- ✓ ...
- ✓ bullet cluster 1E0657-558



rotational curve of
a spiral galaxy

bullet cluster



$M_{\text{visible Universe}} \ll M_{\text{gravitational effect}} \Rightarrow$ about 90% of the mass is **DARK**

“Concordance Λ CDM model”

$$\Omega = \Omega_{\Lambda} + \Omega_M = \text{close to 1}$$

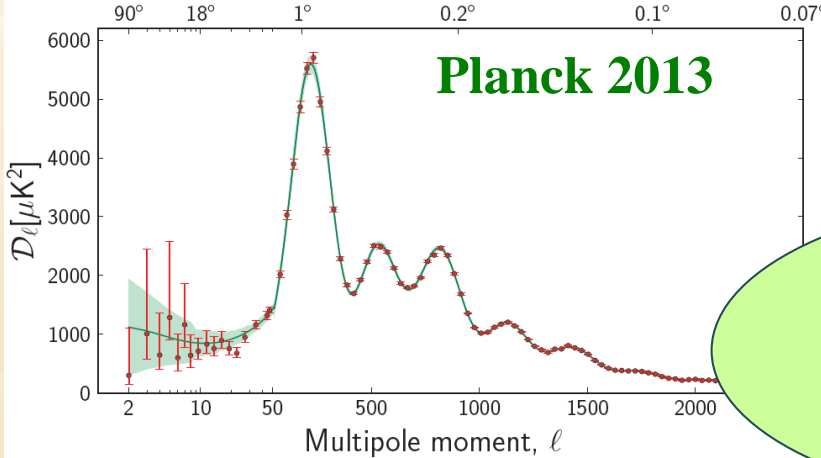
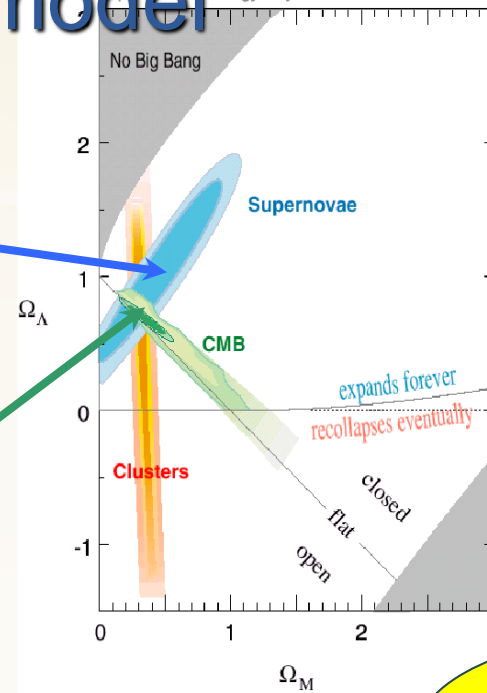
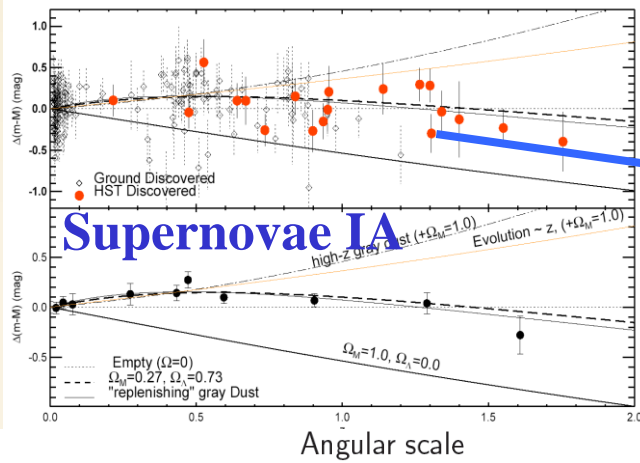
$\Omega = \text{density/critical density}$

6 atoms of H/m^3

$$\Omega_{\Lambda} \approx 0.69$$

$$\Omega_M \approx 0.31$$

The Universe is **flat**



- Observations on:
- light nuclei abundance
 - microlensings
 - visible light.

Primordial Nucleosynthesis

Structure formation in the Universe

The baryons give “too small” contribution

$$\Omega_b \sim 5\%$$

Non baryonic Cold Dark Matter is dominant

$$\Omega_{\text{CDM}} \sim 27\%,$$

$$\Omega_{\text{HDM}, \nu} < 1\%$$

~ 90% of the matter in the Universe is non baryonic

A large part of the Universe is in form of non baryonic Cold Dark Matter particles

Relic DM particles from primordial Universe



Moreover, several questions arise about:

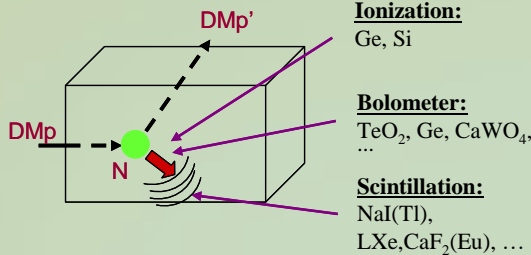
- interaction type with ordinary matter and its description
- related nuclear and particle physics
- halo model and parameters
- halo composition. DM multicomponent also in the particle sector?
- non thermalized components?
- caustics?
- clumpiness?
- etc.



Some direct detection processes:

- Scatterings on nuclei

→ detection of nuclear recoil energy



- Inelastic Dark Matter: $W + N \rightarrow W^* + N$

→ W has Two mass states χ^+ , χ^- with δ mass splitting

→ Kinematical constraint for the inelastic scattering of χ^- on a nucleus

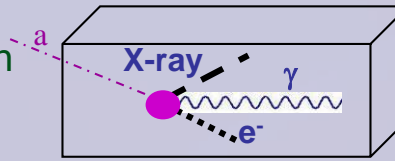
$$\frac{1}{2} \mu v^2 \geq \delta \Leftrightarrow v \geq v_{thr} = \sqrt{\frac{2\delta}{\mu}}$$

- Excitation of bound electrons in scatterings on nuclei

→ detection of recoil nuclei + e.m. radiation

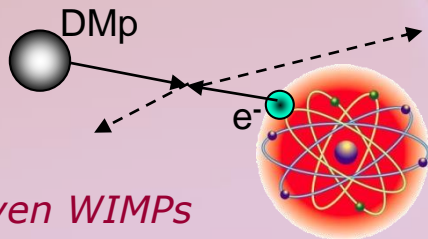
- Conversion of particle into e.m. radiation

→ detection of γ , X-rays, e^-



- Interaction only on atomic electrons

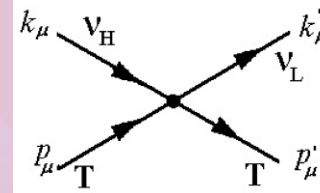
→ detection of e.m. radiation



- Interaction of light DMp (LDM) on e^- or nucleus with production of a lighter particle

→ detection of electron/nucleus recoil energy

e.g. sterile ν



... also other ideas ...

e.g. signals from these candidates are **completely lost** in experiments based on "rejection procedures" of the e.m. component of their rate

- ... and more

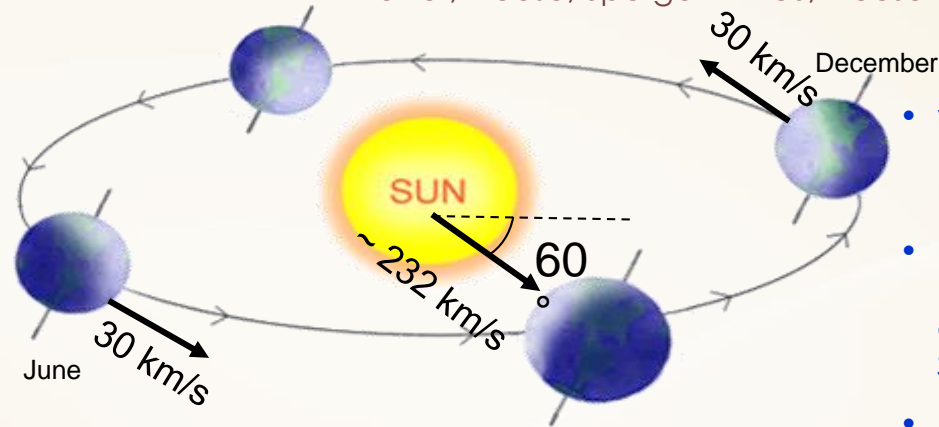
The annual modulation: a model independent signature for the investigation of DM particles component in the galactic halo

With the present technology, the annual modulation is the main model independent signature for the DM signal. Although the modulation effect is expected to be relatively small a suitable large-mass, low-radioactive set-up with an efficient control of the running conditions can point out its presence.

Drukier, Freese, Spergel PRD86; Freese et al. PRD88

Requirements of the annual modulation

- 1) Modulated rate according cosine
- 2) In a definite low energy range
- 3) With a proper period (1 year)
- 4) With proper phase (about 2 June)
- 5) Just for single hit events in a multi-detector set-up
- 6) With modulation amplitude in the region of maximal sensitivity must be <7% for usually adopted halo distributions, but it can be larger in case of some possible scenarios



- $v_{\text{sun}} \sim 232 \text{ km/s}$ (Sun vel in the halo)
- $v_{\text{orb}} = 30 \text{ km/s}$ (Earth vel around the Sun)
- $\gamma = \pi/3$, $\omega = 2\pi/T$, $T = 1 \text{ year}$
- $t_0 = 2^{\text{nd}} \text{ June}$ (when v_{\oplus} is maximum)

$$v_{\oplus}(t) = v_{\text{sun}} + v_{\text{orb}} \cos\gamma \cos[\omega(t-t_0)]$$

$$S_k[\eta(t)] = \int_{\Delta E_k} \frac{dR}{dE_R} dE_R \cong S_{0,k} + S_{m,k} \cos[\omega(t-t_0)]$$

the DM annual modulation signature has a different origin and peculiarities (e.g. the phase) than those effects correlated with the seasons

To mimic this signature, spurious effects and side reactions must not only - obviously - be able to account for the whole observed modulation amplitude, but also to satisfy contemporaneously all the requirements

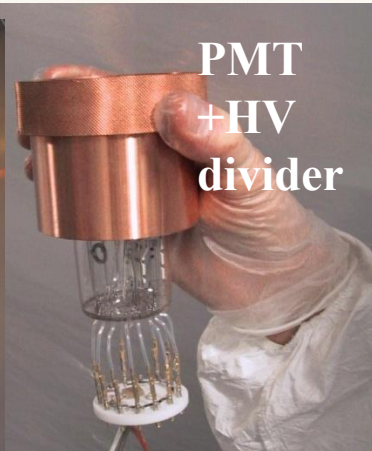
DAMA/LIBRA ~250 kg ULB NaI(Tl) **(Large sodium Iodide Bulk for RARE processes)**



As a result of a second generation R&D for more radiopure NaI(Tl)
by exploiting new chemical/physical radiopurification techniques
(all operations involving crystals and PMTs - including photos - in HP Nitrogen atmosphere)



**improving installation
and environment**



**PMT
+HV
divider**

**Cu etching with
super- and ultra-pure
HCl solutions, dried
and sealed in HP N₂**



**etching staff at work
in clean room**



storing new crystals



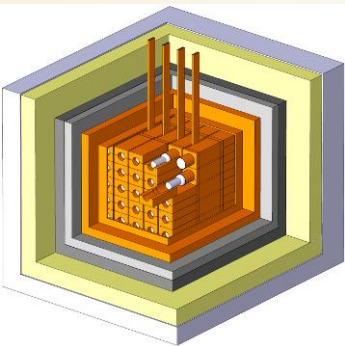
The DAMA/LIBRA set-up

For details, radiopurity, performances, procedures, etc.

NIMA592(2008)297

Polyethylene/paraffin

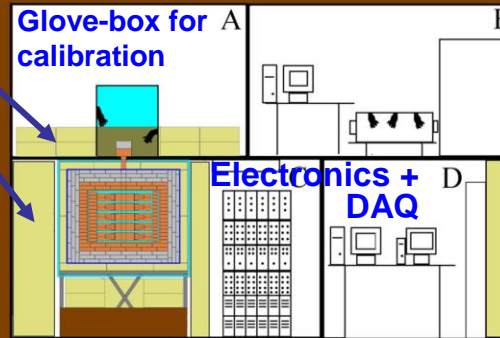
- 25 x 9.7 kg NaI(Tl) in a 5x5 matrix
- two Suprasil-B light guides directly coupled to each bare crystal
- two PMTs working in coincidence at the single ph. el. threshold



5.5-7.5 phe/keV



Installation



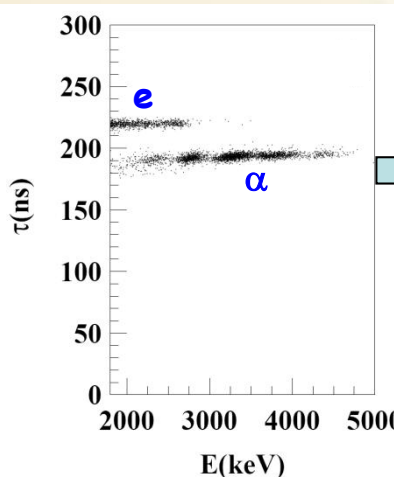
- OFHC low radioactive copper
- Low radioactive lead
- Cadmium foils
- Polyethylene/Paraffin
- Concrete from GS rock



- ~ 1m concrete from GS rock
- Dismounting/Installing protocol (with "Scuba" system)
- All the materials selected for low radioactivity
- Multicomponent passive shield (>10 cm of Cu, 15 cm of Pb + Cd foils, 10/40 cm Polyethylene/paraffin, about 1 m concrete, mostly outside the installation)
- Three-level system to exclude Radon from the detectors
- Calibrations in the same running conditions as production runs
- Installation in air conditioning + huge heat capacity of shield
- Monitoring/alarm system; many parameters acquired with the production data
- Pulse shape recorded by Waweform Analyzer Acqiris DC270 (2chs per detector), 1 Gsample/s, 8 bit, bandwidth 250 MHz
- Data collected from low energy up to MeV region, despite the hardware optimization was done for the low energy



Some on residual contaminants in new ULB NaI(Tl) detectors



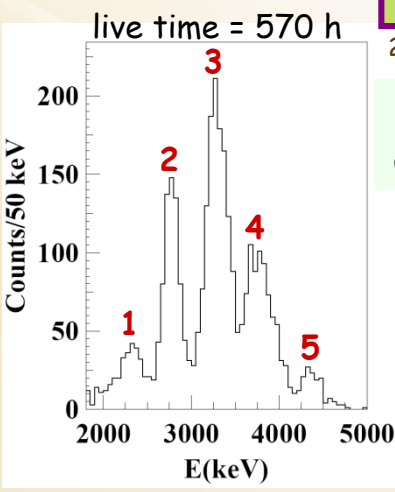
α/e pulse shape discrimination has practically 100% effectiveness in the MeV range

The measured α yield in the new DAMA/LIBRA detectors ranges from 7 to some tens α /kg/day

Second generation R&D for new DAMA/LIBRA crystals: new selected powders, physical/chemical radiopurification, new selection of overall materials, new protocol for growing and handling

^{232}Th residual contamination From time-amplitude method. If ^{232}Th chain at equilibrium: it ranges from 0.5 ppt to 7.5 ppt

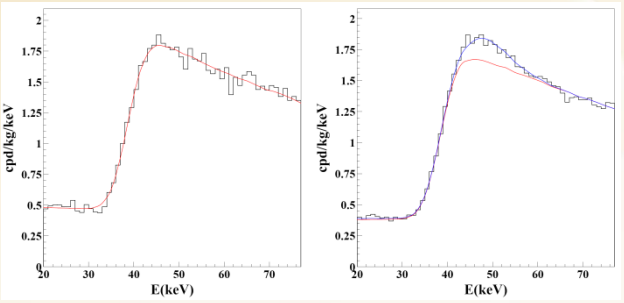
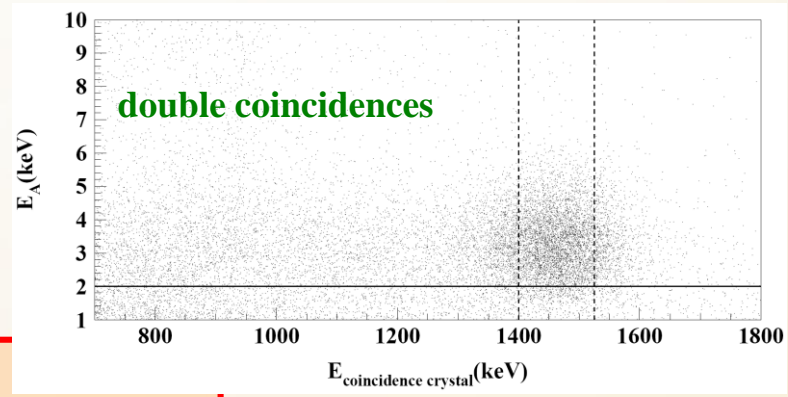
^{238}U residual contamination First estimate: considering the measured α and ^{232}Th activity, if ^{238}U chain at equilibrium \Rightarrow ^{238}U contents in new detectors typically range from 0.7 to 10 ppt



^{238}U chain splitted into 5 subchains: $^{238}\text{U} \rightarrow ^{234}\text{U} \rightarrow ^{230}\text{Th} \rightarrow ^{226}\text{Ra} \rightarrow ^{210}\text{Pb} \rightarrow ^{206}\text{Pb}$

Thus, in this case: (2.1 ± 0.1) ppt of ^{232}Th ; (0.35 ± 0.06) ppt for ^{238}U
 and: (15.8 ± 1.6) $\mu\text{Bq/kg}$ for $^{234}\text{U} + ^{230}\text{Th}$; (21.7 ± 1.1) $\mu\text{Bq/kg}$ for ^{226}Ra ; (24.2 ± 1.6) $\mu\text{Bq/kg}$ for ^{210}Pb .

$^{\text{nat}}\text{K}$ residual contamination
 The analysis has given for the $^{\text{nat}}\text{K}$ content in the crystals values not exceeding about 20 ppb



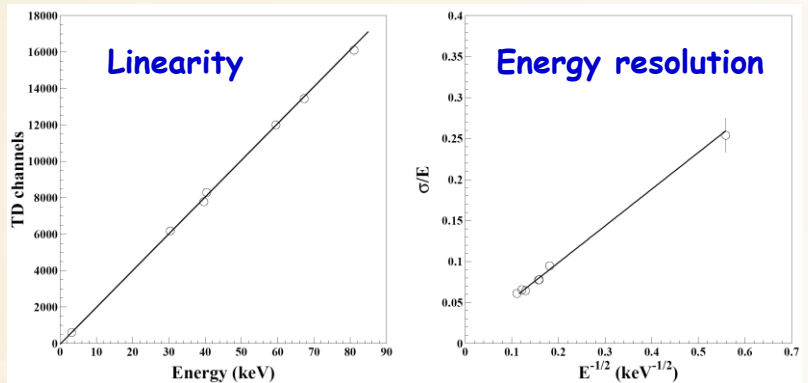
^{129}I and ^{210}Pb
 $^{129}\text{I}/^{\text{nat}}\text{I} \approx 1.7 \times 10^{-13}$ for all the new detectors
 ^{210}Pb in the new detectors: $(5 - 30)$ $\mu\text{Bq/kg}$.

No sizable surface pollution by Radon daughters, thanks to the new handling protocols

... more on NIMA592(2008)297

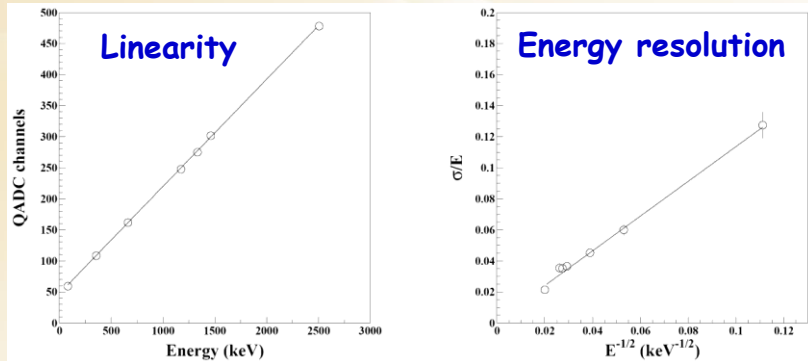
DAMA/LIBRA calibrations

Low energy: various external gamma sources (^{241}Am , ^{133}Ba) and internal X-rays or gamma's (^{40}K , ^{125}I , ^{129}I), routine calibrations with ^{241}Am



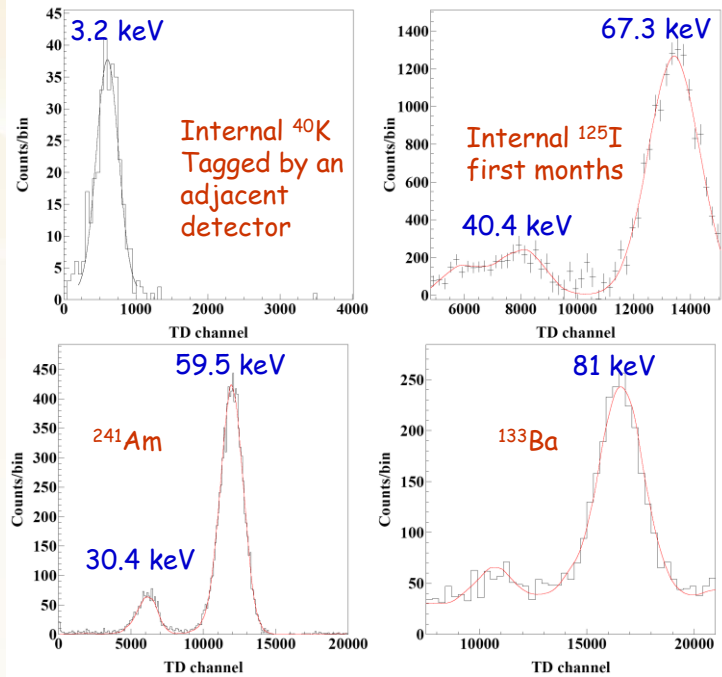
$$\frac{\sigma_{LE}}{E} = \frac{(0.448 \pm 0.035)}{\sqrt{E(\text{keV})}} + (9.1 \pm 5.1) \cdot 10^{-3}$$

High energy: external sources of gamma rays (e.g. ^{137}Cs , ^{60}Co and ^{133}Ba) and gamma rays of 1461 keV due to ^{40}K decays in an adjacent detector, tagged by the 3.2 keV X-rays

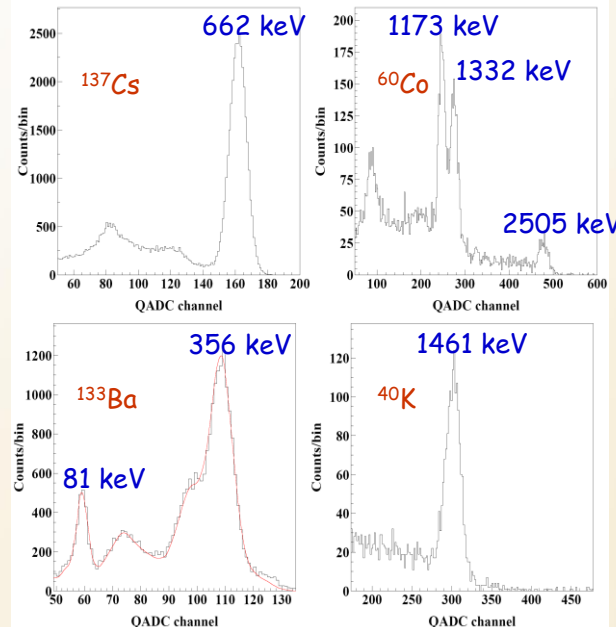


$$\frac{\sigma_{HE}}{E} = \frac{(1.12 \pm 0.06)}{\sqrt{E(\text{keV})}} + (17 \pm 23) \cdot 10^{-4}$$

Thus, here and hereafter keV means keV electron equivalent



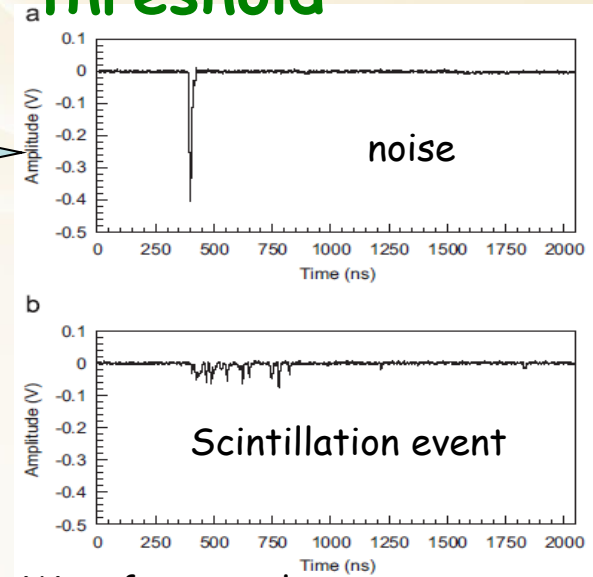
The curves superimposed to the experimental data have been obtained by simulations



The signals (unlike low energy events) for high energy events are taken from one PMT

Noise rejection near the energy threshold

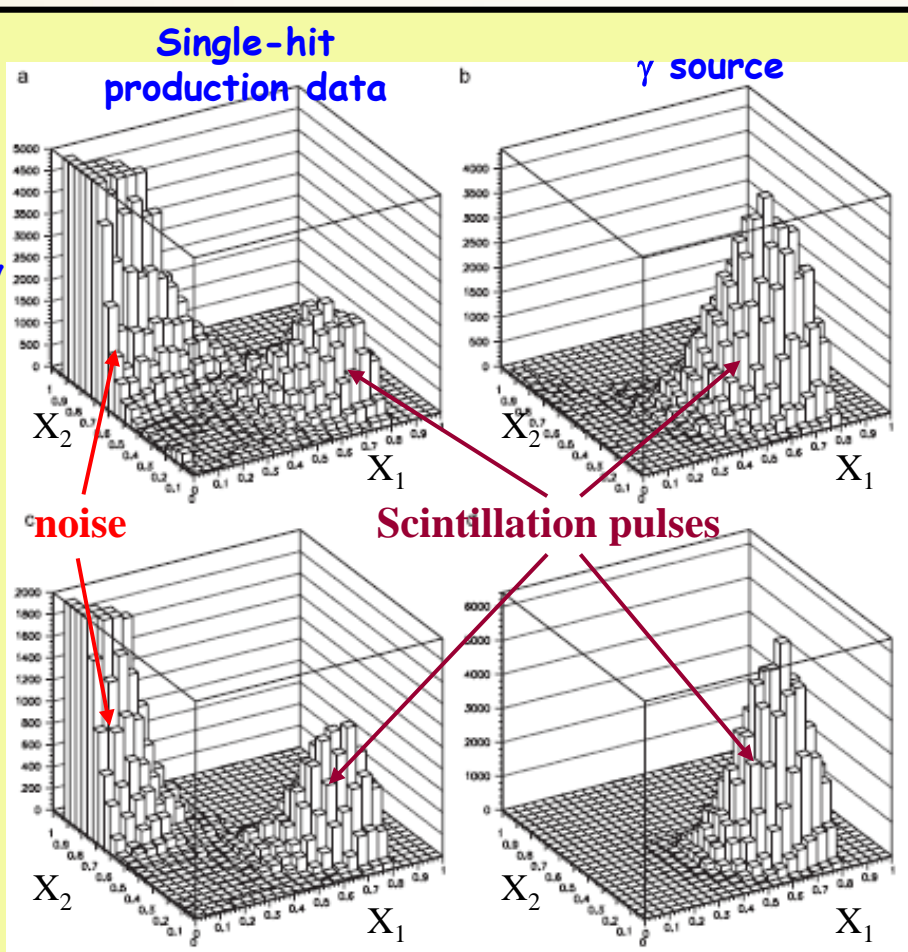
Typical pulse profiles of noise and of scintillation event with the same area, just above the energy threshold of 2 keV



The different time characteristics of noise (decay time of order of tens of ns) and of scintillation event (decay time about 240 ns) can be investigated building several variables

2-4 keV

4-6 keV



From the Waveform Analyser
2048 ns time window:

$$X_1 = \frac{\text{Area (from 100 ns to 600 ns)}}{\text{Area (from 0 ns to 600 ns)}}$$

$$X_2 = \frac{\text{Area (from 0 ns to 50 ns)}}{\text{Area (from 0 ns to 600 ns)}}$$

- The separation between noise and scintillation pulses is very good.
- Very clean samples of scintillation events selected by stringent acceptance windows.
- The related efficiencies evaluated by calibrations with ^{241}Am sources of suitable activity in the same experimental conditions and energy range as the production data (efficiency measurements performed each ~10 days; typically 10^4 - 10^5 events per keV collected)

This is the only procedure applied to the analysed data

Complete DAMA/LIBRA-phase1

	Period	Mass (kg)	Exposure (kg×day)	$(\alpha - \beta^2)$
DAMA/LIBRA-1	Sept. 9, 2003 - July 21, 2004	232.8	51405	0.562
DAMA/LIBRA-2	July 21, 2004 - Oct. 28, 2005	232.8	52597	0.467
DAMA/LIBRA-3	Oct. 28, 2005 - July 18, 2006	232.8	39445	0.591
DAMA/LIBRA-4	July 19, 2006 - July 17, 2007	232.8	49377	0.541
DAMA/LIBRA-5	July 17, 2007 - Aug. 29, 2008	232.8	66105	0.468
DAMA/LIBRA-6	Nov. 12, 2008 - Sept. 1, 2009	242.5	58768	0.519
DAMA/LIBRA-7	Sept. 1, 2009 - Sept. 8, 2010	242.5	62098	0.515
DAMA/LIBRA-phase1	Sept. 9, 2003 - Sept. 8, 2010		379795 \simeq 1.04 ton×yr	0.518
DAMA/NaI + DAMA/LIBRA-phase1:			1.33 ton×yr	

a ton × yr experiment? done

- EPJC56(2008)333
- EPJC67(2010)39
- EPJC73(2013)2648
- calibrations: \approx 96 M events from sources
- acceptance window eff: 95 M events (\approx 3.5 M events/keV)

• First upgrade on Sept 2008:

- replacement of some PMTs in HP N₂ atmosphere
- restore 1 detector to operation
- new Digitizers installed (U1063A Acqiris 1GS/s 8-bit High-Speed cPCI)
- new DAQ system with optical read-out installed

START of DAMA/LIBRA – phase 2

• Second upgrade on Oct./Nov. 2010

- ✧ Replacement of all the PMTs with higher Q.E. ones from dedicated developments
- ✧ Goal: lowering the software energy threshold

Fall 2012: new preamplifiers installed + special trigger modules. Other new components in the electronic chain in development



... continuously running

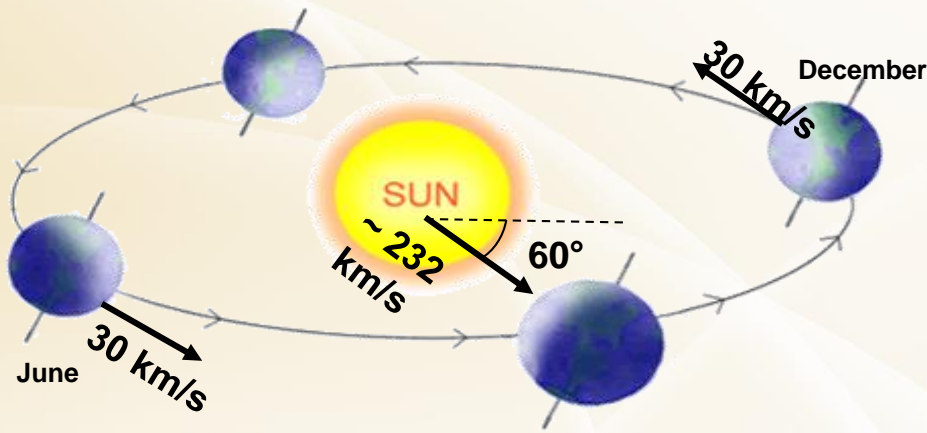


Experimental *single-hit* residuals rate vs time and energy

- Model-independent investigation of the annual modulation signature has been carried out by exploiting the time behaviour of the residual rates of the *single-hit* events in the lowest energy regions of the DAMA/LIBRA data.
- These residual rates are calculated from the measured rate of the *single-hit* events (obviously corrections for the overall efficiency and for the acquisition dead time are already applied) after subtracting the constant part:



$$\left\langle r_{ijk} - flat_{jk} \right\rangle_{jk}$$



- r_{ijk} is the rate in the considered i -th time interval for the j -th detector in the k -th energy bin
- $flat_{jk}$ is the rate of the j -th detector in the k -th energy bin averaged over the cycles.
- The average is made on all the detectors (j index) and on all the energy bins (k index)
- The weighted mean of the residuals must obviously be zero over one cycle.

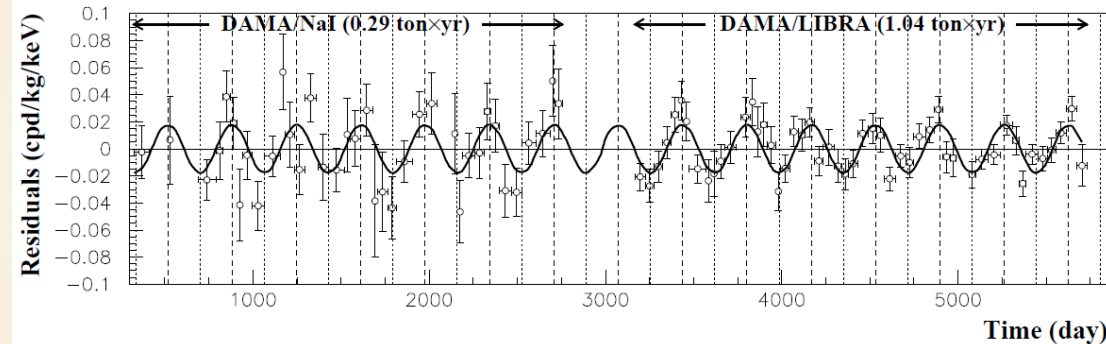
Model Independent DM Annual Modulation Result

experimental residuals of the single-hit scintillation events rate vs time and energy

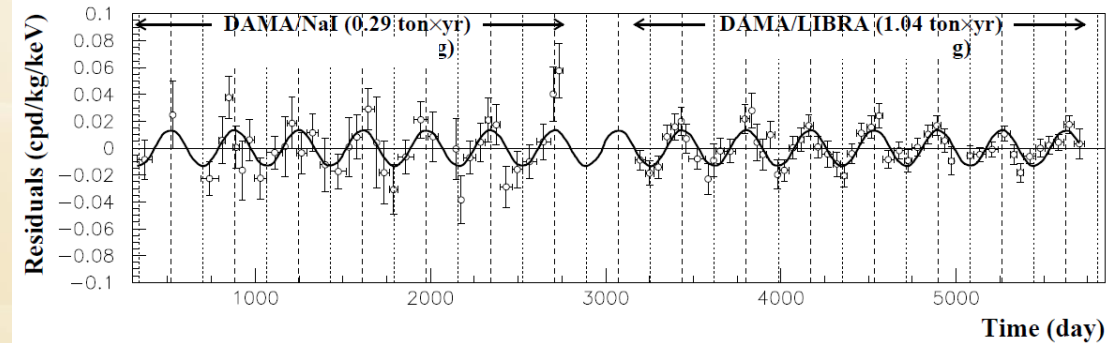
DAMA/NaI + DAMA/LIBRA-phase1

Total exposure: 487526 kg×day = 1.33 ton×yr

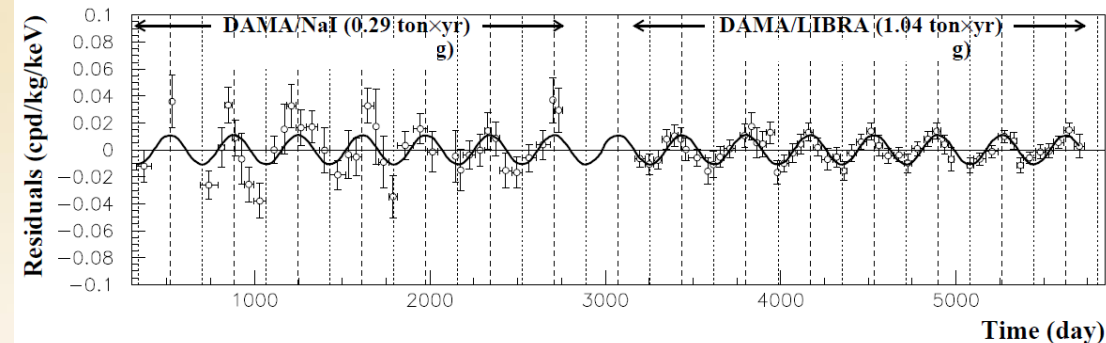
2-4 keV



2-5 keV



2-6 keV



$\text{Acos}[\omega(t-t_0)]$;
continuous lines: $t_0 = 152.5$ d, $T = 1.00$ y

2-4 keV

$A = (0.0179 \pm 0.0020)$ cpd/kg/keV

$\chi^2/\text{dof} = 87.1/86$ **9.0 σ C.L.**

Absence of modulation? No

$\chi^2/\text{dof} = 169/87 \Rightarrow P(A=0) = 3.7 \times 10^{-7}$

2-5 keV

$A = (0.0135 \pm 0.0015)$ cpd/kg/keV

$\chi^2/\text{dof} = 68.2/86$ **9.0 σ C.L.**

Absence of modulation? No

$\chi^2/\text{dof} = 152/87 \Rightarrow P(A=0) = 2.2 \times 10^{-5}$

2-6 keV

$A = (0.0110 \pm 0.0012)$ cpd/kg/keV

$\chi^2/\text{dof} = 70.4/86$ **9.2 σ C.L.**

Absence of modulation? No

$\chi^2/\text{dof} = 154/87 \Rightarrow P(A=0) = 1.3 \times 10^{-5}$

The data favor the presence of a modulated behavior with proper features at 9.2 σ C.L.

Modulation amplitudes (A), period (T) and phase (t_0) measured in DAMA/NaI and DAMA/LIBRA-phase1

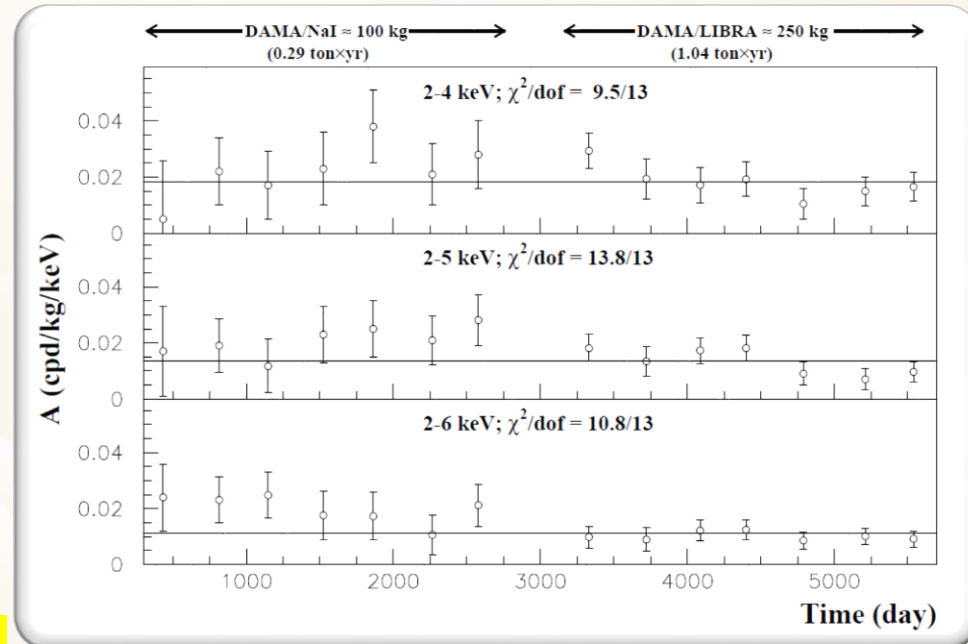
DAMA/NaI (0.29 ton x yr) + DAMA/LIBRA-phase1 (1.04 ton x yr)

total exposure: 487526 kg×day = 1.33 ton×yr

$$\text{Acos}[\omega(t-t_0)]$$

	A(cpd/kg/keV)	T=2 π / ω (yr)	t_0 (day)	C.L.
DAMA/NaI+DAMA/LIBRA-phase1				
(2-4) keV	0.0190 ±0.0020	0.996 ±0.0002	134 ± 6	9.5 σ
(2-5) keV	0.0140 ±0.0015	0.996 ±0.0002	140 ± 6	9.3 σ
(2-6) keV	0.0112 ±0.0012	0.998 ±0.0002	144 ± 7	9.3 σ

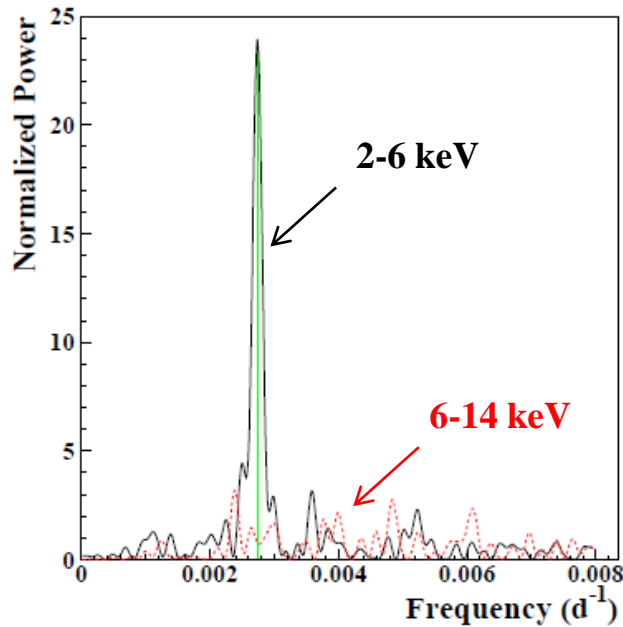
χ^2 test ($\chi^2 = 9.5, 13.8$ and 10.8 over 13 d.o.f. for the three energy intervals, respectively; upper tail probability 73%, 39%, 63%) and *run test* (lower tail probabilities of 41%, 29% and 23% for the three energy intervals, respectively) **accept** at 90% C.L. the hypothesis that the modulation amplitudes are normally fluctuating around their best fit values.



Compatibility among the annual cycles

Power spectrum of single-hit residuals

DAMA/NaI (7 years) + DAMA/LIBRA-phase1 (7 years)
total exposure: 1.33 ton×yr



Principal mode in the 2-6 keV region:
 $2.737 \times 10^{-3} \text{ d}^{-1} \approx 1 \text{ yr}^{-1}$

Not present in the 6-14 keV
region (only aliasing peaks)

The Lomb-Scargle periodogram, as reported in DAMA papers, always according to Ap.J. 263 (1982) 835, Ap.J. 338 (1989) 277 with the treatment of the experimental errors and of the time binning:

Given a set of data values r_i , $i = 1, \dots, N$ at respective observation times t_i , the Lomb-Scargle periodogram is:

$$P_N(\omega) = \frac{1}{2\sigma^2} \left\{ \frac{\left[\sum_i (r_i - \bar{r}) \cos \omega(t_i - \tau) \right]^2}{\sum_i \cos^2 \omega(t_i - \tau)} + \frac{\left[\sum_i (r_i - \bar{r}) \sin \omega(t_i - \tau) \right]^2}{\sum_i \sin^2 \omega(t_i - \tau)} \right\}$$

where: $\bar{r} = \frac{1}{N} \sum_1^N r_i$ $\sigma^2 = \frac{1}{N-1} \sum_1^N (r_i - \bar{r})^2$

and, for each angular frequency $\omega = 2\pi f > 0$ of interest, the time-offset τ is:

$$\tan(2\omega\tau) = \frac{\sum_i \sin(2\omega t_i)}{\sum_i \cos(2\omega t_i)}$$

The Nyquist frequency is $\approx 3 \text{ yr}^{-1}$ ($\approx 0.008 \text{ d}^{-1}$); meaningless higher frequencies, washed off by the integration over the time binning.

In order to take into account the different time binning and the residuals' errors we have to rewrite the previous formulae replacing:

$$\sum_i \rightarrow \sum_i \frac{\frac{N}{\Delta t_i^2}}{\sum_j \frac{1}{\Delta t_j^2}} = \frac{N}{\sum_j \frac{1}{\Delta t_j^2}} \cdot \sum_i \frac{1}{\Delta t_i^2}$$

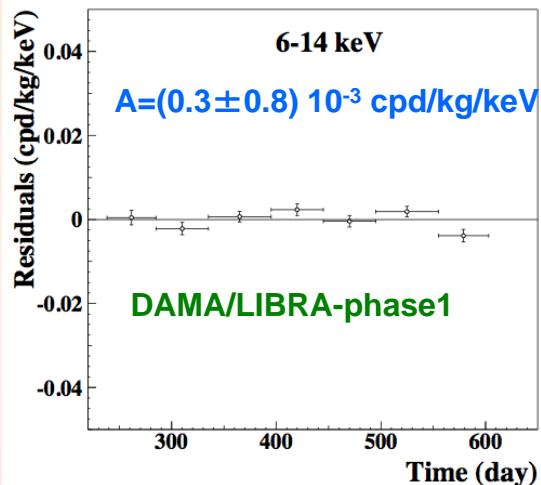
$$\sin \omega t_i \rightarrow \frac{1}{2\Delta t_i} \int_{t_i - \Delta t_i}^{t_i + \Delta t_i} \sin \omega t \, dt$$

$$\cos \omega t_i \rightarrow \frac{1}{2\Delta t_i} \int_{t_i - \Delta t_i}^{t_i + \Delta t_i} \cos \omega t \, dt$$

Clear annual modulation is evident in (2-6) keV, while it is absent just above 6 keV

Rate behaviour above 6 keV

• No Modulation above 6 keV

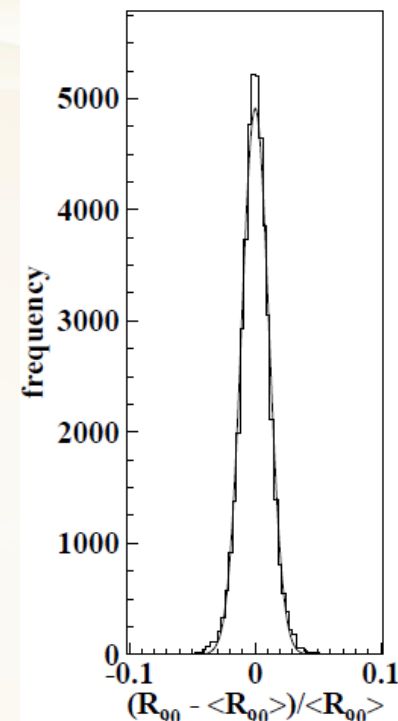


Mod. Ampl. (6-10 keV): cpd/kg/keV

- (0.0016 ± 0.0031) DAMA/LIBRA-1
- (0.0010 ± 0.0034) DAMA/LIBRA-2
- (0.0001 ± 0.0031) DAMA/LIBRA-3
- (0.0006 ± 0.0029) DAMA/LIBRA-4
- (0.0021 ± 0.0026) DAMA/LIBRA-5
- (0.0029 ± 0.0025) DAMA/LIBRA-6
- (0.0023 ± 0.0024) DAMA/LIBRA-7

→ statistically consistent with zero

DAMA/LIBRA-phase1



$\sigma \approx 1\%$, fully accounted by statistical considerations

• No modulation in the whole energy spectrum:

studying integral rate at higher energy, R_{90}

- R_{90} percentage variations with respect to their mean values for single crystal in the DAMA/LIBRA running periods
- Fitting the behaviour with time, adding a term modulated with period and phase as expected for DM particles:

consistent with zero

Period	Mod. Ampl.
DAMA/LIBRA-1	$-(0.05 \pm 0.19)$ cpd/kg
DAMA/LIBRA-2	$-(0.12 \pm 0.19)$ cpd/kg
DAMA/LIBRA-3	$-(0.13 \pm 0.18)$ cpd/kg
DAMA/LIBRA-4	(0.15 ± 0.17) cpd/kg
DAMA/LIBRA-5	(0.20 ± 0.18) cpd/kg
DAMA/LIBRA-6	$-(0.20 \pm 0.16)$ cpd/kg
DAMA/LIBRA-7	$-(0.28 \pm 0.18)$ cpd/kg

+ if a modulation present in the whole energy spectrum at the level found in the lowest energy region → $R_{90} \sim \text{tens cpd/kg}$ → $\sim 100 \sigma$ far away

No modulation above 6 keV

This accounts for all sources of bckg and is consistent with the studies on the various components

Multiple-hits events in the region of the signal

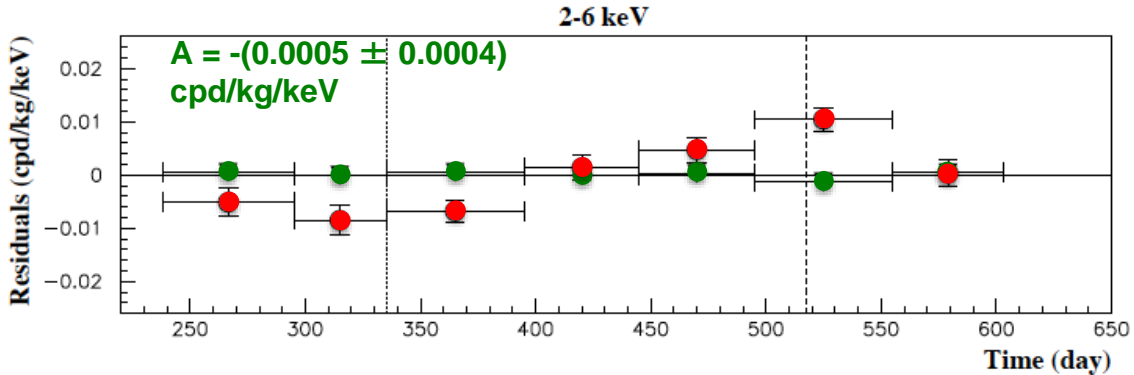
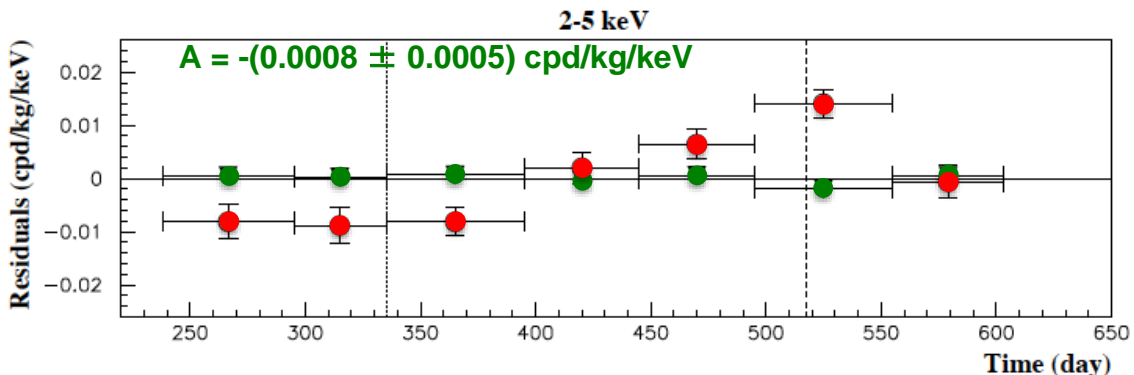
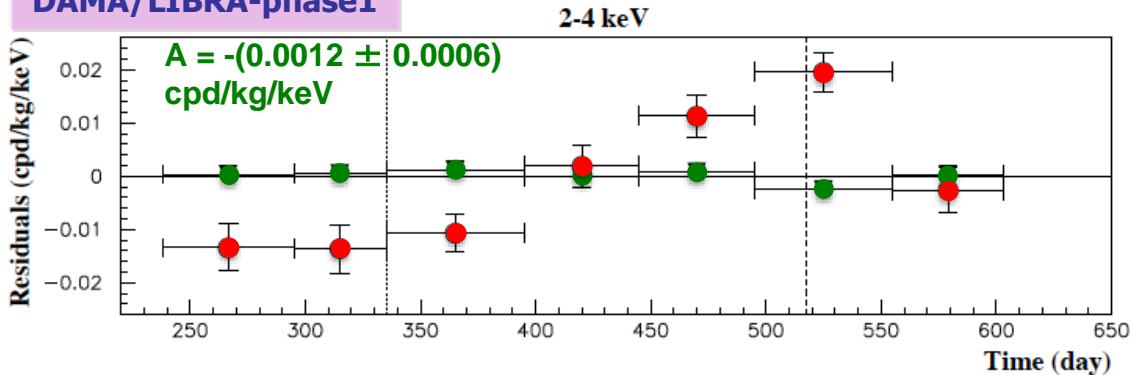
- Each detector has its own TDs read-out → pulse profiles of *multiple-hits* events (multiplicity > 1) acquired (exposure: 1.04 ton×yr).
- The same hardware and software procedures as those followed for *single-hit* events

signals by Dark Matter particles do not belong to *multiple-hits* events, that is:

multiple-hits events = Dark Matter particles events "switched off"

- Evidence of annual modulation with proper features as required by the DM annual modulation signature:
- present in the *single-hit* residuals
 - absent in the *multiple-hits* residual

DAMA/LIBRA-phase1



This result offers an additional strong support for the presence of Dark Matter particles in the galactic halo, further excluding any side effect either from hardware or from software procedures or from background

Modulation amplitudes, $S_{m,k}$, as function of the energy

The likelihood function of the *single-hit* experimental data in the k -th energy bin is defined as:

$$L_k = \prod_{ij} e^{-\mu_{ijk}} \frac{\mu_{ijk}^{N_{ijk}}}{N_{ijk}!}$$

N_{ijk} is the number of events collected in the i -th time interval, by the j -th detector and in the k -th energy bin.

N_{ijk} follows a Poissonian distribution with expectation value:

$$\mu_{ijk} = [b_{jk} + R_k(t)] M_j \Delta t_i \Delta E \varepsilon_{jk} = [b_{jk} + S_{0,k} + S_{m,k} \cos \omega(t_i - t_0)] M_j \Delta t_i \Delta E \varepsilon_{jk}$$

The b_{jk} are the background contributions, M_j is the mass of the j -th detector, Δt_i is the detector running time during the i -th time interval, ΔE is the chosen energy bin, ε_{jk} is the overall efficiency.

The usual procedure is to minimize the function $y_k = -2 \ln(L_k) - \text{const}$ for each energy bin; the free parameters of the fit are the $(b_{jk} + S_{0,k})$ contributions and the $S_{m,k}$ parameter.

The $S_{m,k}$ is the modulation amplitude of the modulated part of the signal obtained by maximum likelihood method over the data considering $T = 2\pi/\omega = 1 \text{ yr}$ and $t_0 = 152.5 \text{ day}$.

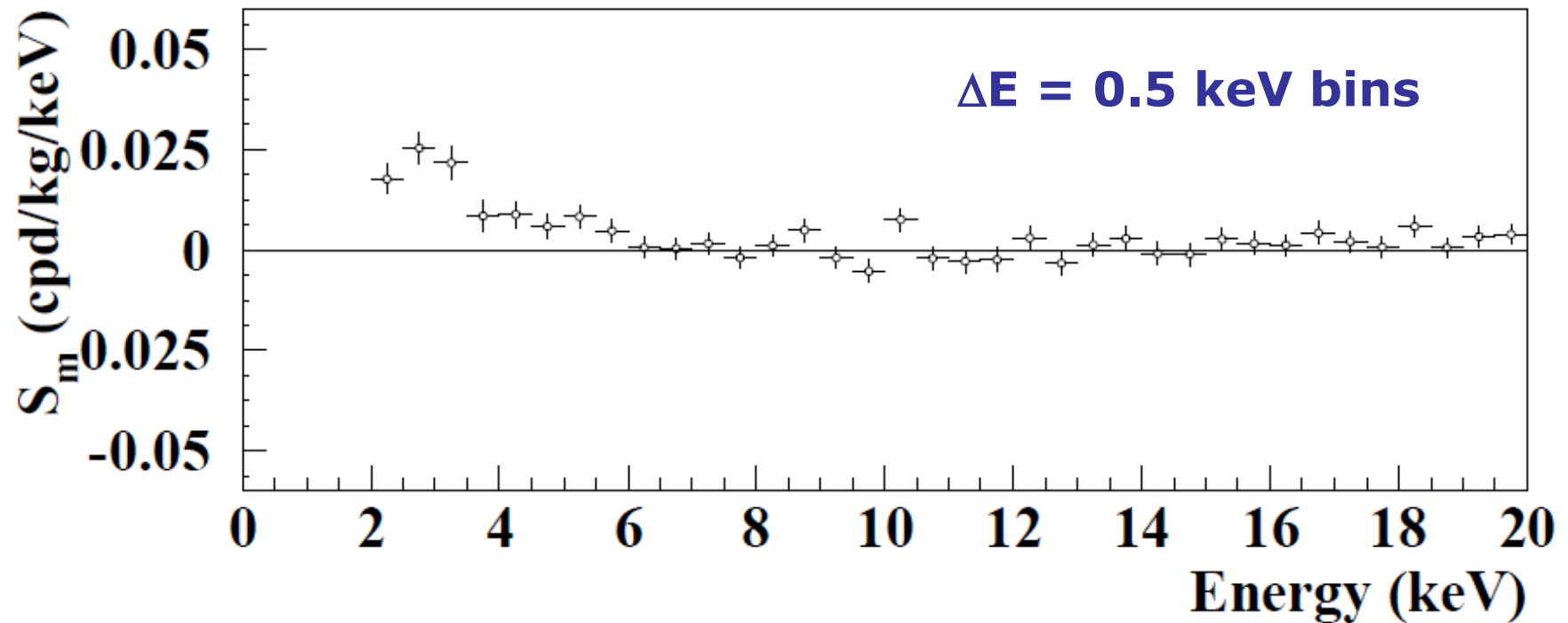
Energy distribution of the modulation amplitudes

$$R(t) = S_0 + S_m \cos(\omega(t - t_0))$$

here $T = 2\pi/\omega = 1$ yr and $t_0 = 152.5$ day

DAMA/NaI + DAMA/LIBRA-phase1

total exposure: 487526 kg×day \approx **1.33 ton×yr**



A clear modulation is present in the (2-6) keV energy interval, while S_m values compatible with zero are present just above

The S_m values in the (6-20) keV energy interval have random fluctuations around zero with χ^2 equal to 35.8 for 28 degrees of freedom (upper tail probability 15%)

Final model independent result DAMA/NaI + DAMA/LIBRA-phase1

- Presence of modulation for 14 annual cycles at 9.3σ C.L. with the proper distinctive features of the DM signature; all the features satisfied by the data over 14 independent experiments of 1 year each one
- The total exposure by former DAMA/NaI and present DAMA/LIBRA is $1.33 \text{ ton} \times \text{yr}$ (14 annual cycles)
- In fact, as required by the DM annual modulation signature:

1. The *single-hit* events show a clear cosine-like modulation, as expected for the DM signal

2. Measured period is equal to (0.998 ± 0.002) yr, well compatible with the 1 yr period, as expected for the DM signal

3. Measured phase (144 ± 7) days is well compatible with 152.5 days, as expected for the DM signal

4. The modulation is present only in the low energy (2-6) keV interval and not in other higher energy regions, consistently with expectation for the DM signal

5. The modulation is present only in the *single-hit* events, while it is absent in the *multiple-hits*, as expected for the DM signal

6. The measured modulation amplitude in NaI(Tl) of the *single-hit* events in (2-6) keV is:
 (0.0112 ± 0.0012) cpd/kg/keV (9.3σ C.L.).

No systematic or side process able to simultaneously satisfy all the many peculiarities of the signature and to account for the whole measured modulation amplitude is available

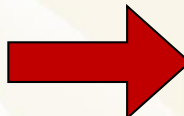
Summary of the results obtained in the additional investigations of possible systematics or side reactions

(NIMA592(2008)297, EPJC56(2008)333, arXiv:0912.0660, Can. J. Phys. 89 (2011) 11, S.I.F. Atti Conf.103(211) (arXiv:1007.0595), PhysProc37(2012)1095, EPJC72(2012)2064 and refs therein)

Source	Main comment	Cautious upper limit (90%C.L.)
RADON	Sealed Cu box in HP Nitrogen atmosphere, 3-level of sealing, etc.	$<2.5 \times 10^{-6}$ cpd/kg/keV
TEMPERATURE	Installation is air conditioned+ detectors in Cu housings directly in contact with multi-ton shield → huge heat capacity + T continuously recorded	$<10^{-4}$ cpd/kg/keV
NOISE	Effective full noise rejection near threshold	$<10^{-4}$ cpd/kg/keV
ENERGY SCALE	Routine + intrinsic calibrations	$<1-2 \times 10^{-4}$ cpd/kg/keV
EFFICIENCIES	Regularly measured by dedicated calibrations	$<10^{-4}$ cpd/kg/keV
BACKGROUND	No modulation above 6 keV; no modulation in the (2-6) keV <i>multiple-hits</i> events; this limit includes all possible sources of background	$<10^{-4}$ cpd/kg/keV
SIDE REACTIONS	Muon flux variation measured at LNGS	$<3 \times 10^{-5}$ cpd/kg/keV



+ they cannot satisfy all the requirements of annual modulation signature



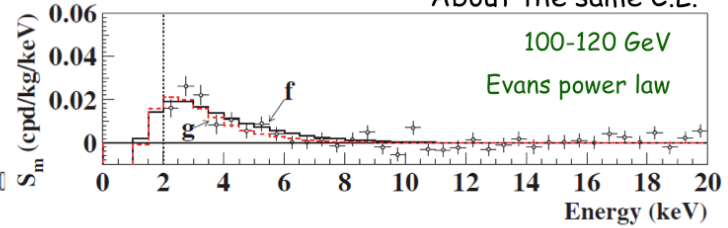
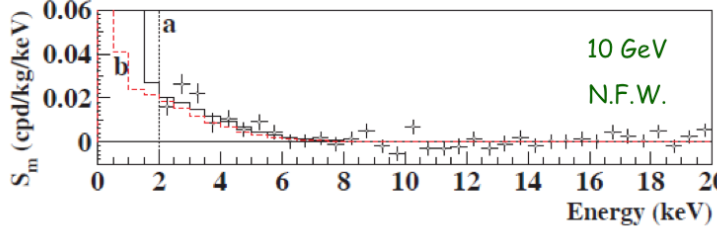
Thus, they cannot mimic the observed annual modulation effect

Model-independent evidence by DAMA/NaI and DAMA/LIBRA

well compatible with several candidates in many astrophysical, nuclear and particle physics scenarios

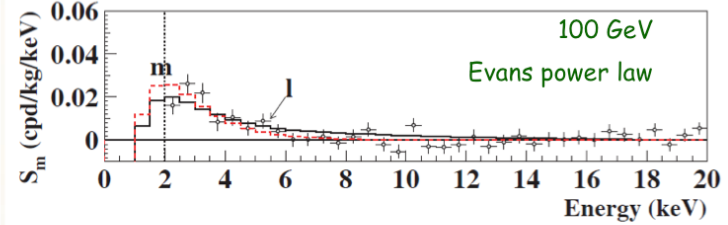
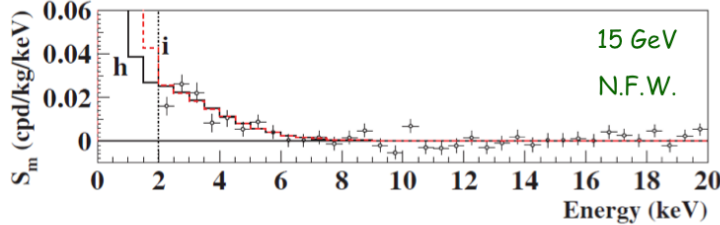
Just few examples of interpretation of the annual modulation in terms of candidate particles in some scenarios

WIMP: SI

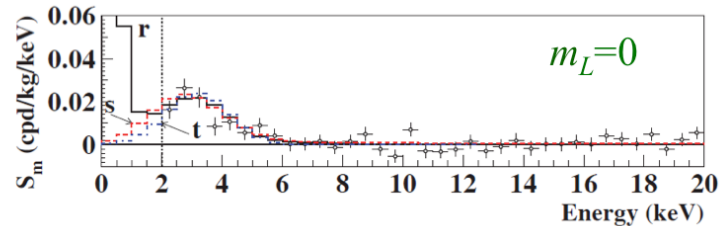
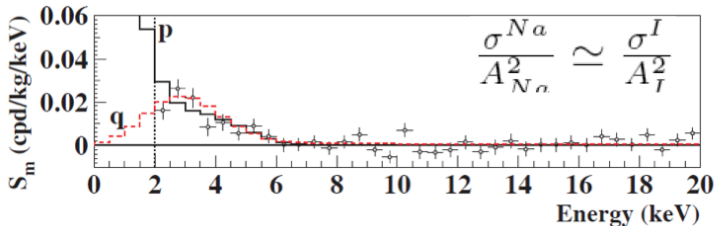


- Not best fit
- About the same C.L.

WIMP: SI & SD $\theta = 2.435$



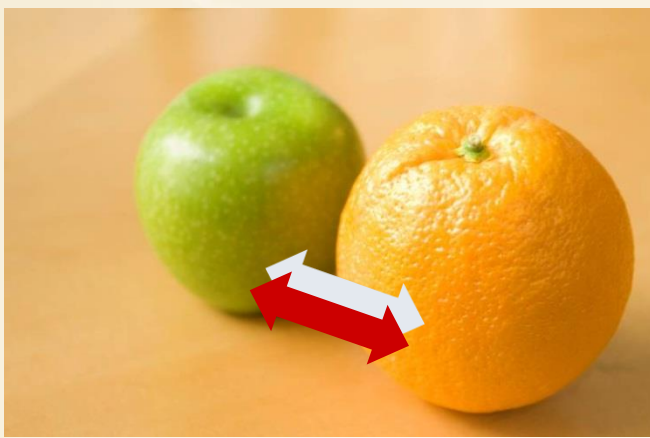
LDM, bosonic DM



Compatibility with several candidates;
other ones are open

About interpretation

See e.g.: Riv.N.Cim.26 n.1(2003)1, TJMPD13(2004)2127, EPJC47(2006)263, IJMPA21(2006)1445, EPJC56(2008)333, PRD84(2011)055014, IJMPA28(2013)1330022



...models...

- Which particle?
- Which interaction coupling?
- Which Form Factors for each target-material?
- Which Spin Factor?
- Which nuclear model framework?
- Which scaling law?
- Which halo model, profile and related parameters?
- Streams?
- ...

...and experimental aspects...

- Exposures
- Energy threshold
- Detector response (phe/keV)
- Energy scale and energy resolution
- Calibrations
- Stability of all the operating conditions.
- Selections of detectors and of data.
- Subtraction/rejection procedures and stability in time of all the selected windows and related quantities
- Efficiencies
- Definition of fiducial volume and non-uniformity
- Quenching factors, channeling, ...
- ...

Uncertainty in experimental parameters, as well as necessary assumptions on various related astrophysical, nuclear and particle-physics aspects, affect all the results at various extent, both in terms of exclusion plots and in terms of allowed regions/volumes. Thus comparisons with a fixed set of assumptions and parameters' values are intrinsically strongly uncertain.

No experiment can be directly compared in model independent way with DAMA

Possible DAMA/LIBRA-phase3

- The light collection of the detectors can further be improved
- Light yields and the energy thresholds will improve accordingly

The strong interest in the low energy range suggests the possibility of a new development of **high Q.E. PMTs** with **increased radiopurity** to directly couple them to the DAMA/LIBRA crystals, **removing** the special radio-pure quartz (Suprasil B) light guides (10 cm long), which act also as optical window.

The presently-reached PMTs features, but not for the same PMT mod.:

- Q.E. around 35-40% @ 420 nm (NaI(Tl) light)
- radiopurity at level of 5 mBq/PMT (^{40}K), 3-4 mBq/PMT (^{232}Th), 3-4 mBq/PMT (^{238}U), 1 mBq/PMT (^{226}Ra), 2 mBq/PMT (^{60}Co).

R&D efforts to obtain PMTs matching the best performances... **feasible**

No longer need for light guides (a 30-40% improvement in the light collection is expected)

